

ANNUAL SUMMARY

Atlantic Hurricane Season of 2007

MICHAEL J. BRENNAN, RICHARD D. KNABB,* MICHELLE MAINELLI,[†] AND TODD B. KIMBERLAIN

NOAA/NWS/NCEP National Hurricane Center, Miami, Florida

(Manuscript received 6 March 2009, in final form 8 June 2009)

ABSTRACT

The 2007 Atlantic hurricane season had 15 named storms, including 14 tropical storms and 1 subtropical storm. Of these, six became hurricanes, including two major hurricanes, Dean and Felix, which reached category 5 intensity (on the Saffir–Simpson hurricane scale). In addition, there were two unnamed tropical depressions. While the number of hurricanes in the basin was near the long-term mean, 2007 became the first year on record with two category 5 landfalls, with Hurricanes Dean and Felix inflicting severe damage on Mexico and Nicaragua, respectively. Dean was the first category 5 hurricane in the Atlantic basin to make landfall in 15 yr, since Hurricane Andrew (1992). In total, eight systems made landfall in the basin during 2007, and the season's tropical cyclones caused approximately 380 deaths. In the United States, one hurricane, one tropical storm, and three tropical depressions made landfall, resulting in 10 fatalities and about \$50 million in damage.

1. Overview

Activity during the 2007 Atlantic hurricane season was near average, with 15 named storms, including 14 tropical storms and 1 subtropical storm. Six of the named storms became hurricanes, with two becoming major hurricanes, corresponding to category 3 or greater on the Saffir–Simpson hurricane scale (Saffir 1973; Simpson 1974). For the 40-yr period 1967–2006, the Atlantic basin averages for named storms, hurricanes, and major hurricanes are 11, 6, and 2, respectively. Even though the number of named storms was above average, many of these systems were short lived and weak. In fact, the 2007 season recorded a total of eight cyclones that lasted 2 days or less, tying the 2005 season for the largest number of such short-lived storms.

In terms of the National Oceanic and Atmospheric Administration (NOAA) accumulated cyclone energy

(ACE) index (Bell et al. 2000), which measures the collective strength and duration of named storms and hurricanes, the season produced about 84% of the 1951–2000 median activity, within the near-normal tercile of activity. This percentage is the lowest observed since 2002, making 2007 the third-lowest Atlantic season in terms of ACE since 1995. Interestingly, while the two years lower than 2007 in terms of ACE (1997 and 2002) were considered El Niño years, 2007 was a La Niña year. During 2007, Bell et al. (2008) note that an unusually strong tropical upper-tropospheric trough (TUTT) over the central North Atlantic during September, paired with a strong and persistent eastern North American ridge during the August–October period, enhanced the vertical wind shear and resulted in anomalous sinking motion over much of the basin (Fig. 1). Although not characteristic of La Niña hurricane seasons, the observed large-scale circulation anomalies likely resulted in a below average ACE, few strong hurricanes, and a large number of weak but short-lived storms.

Atlantic basin tropical cyclones during 2007 had devastating effects, particularly in areas outside of the United States. For the first time on record, two category 5 hurricanes made landfall in the basin during a single season. Dean struck the Yucatan Peninsula of Mexico at category 5 strength in August, and Felix hit northeastern

* Current affiliation: NOAA/NWS, Honolulu, Hawaii.

[†] Current affiliation: NOAA/NWS/NCEP Central Operations, Camp Springs, Maryland.

Corresponding author address: Dr. Michael J. Brennan, National Hurricane Center, 11691 SW 17th St., Miami, FL 33165.
E-mail: michael.j.brennan@noaa.gov

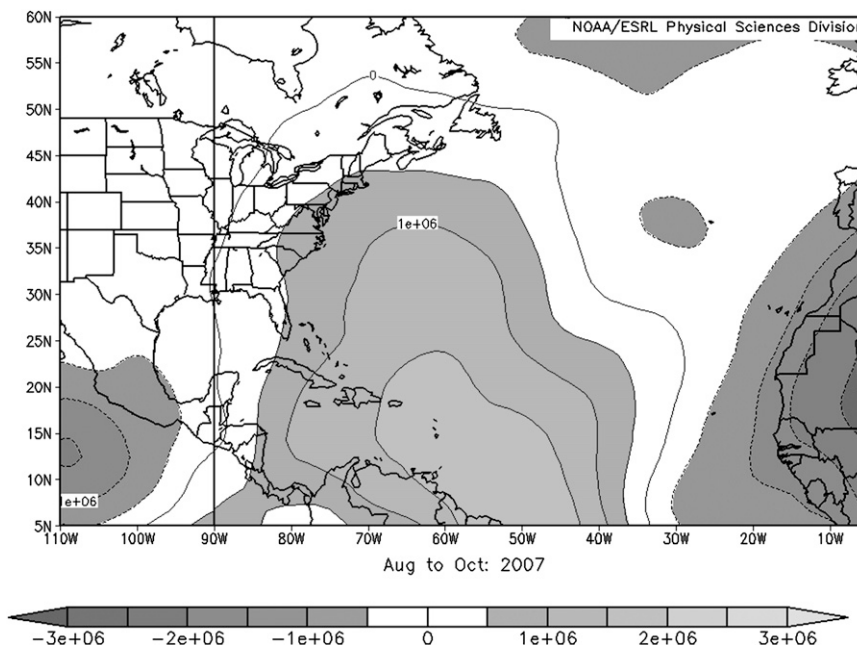


FIG. 1. Composite 0.2101 sigma-level velocity potential anomaly ($\text{m}^2 \text{s}^{-1}$) for August–October 2007 from the National Centers for Environmental Prediction–National Center for Atmospheric Research (NCEP–NCAR) reanalysis dataset (Kalnay et al. 1996). Anomaly is computed from the 1968–96 mean. [Image provided by the NOAA/ESRL Physical Sciences Division, Boulder, CO, from their Web site (<http://www.esrl.noaa.gov/psd/>).]

Nicaragua as a category 5 hurricane in early September. Dean also struck mainland Mexico as a category 2 hurricane, while Lorenzo made landfall in mainland Mexico as a category 1 hurricane in nearly the same location. Noel and Olga caused floods, mudslides, and large loss of life in the Caribbean. The combined death toll from all 2007 Atlantic basin tropical cyclones was about 380. One hurricane, one tropical storm, and three tropical depressions made landfall in the United States, resulting in 10 fatalities and about \$50 million in damages.

2. Individual storm summaries

The individual cyclone summaries in this section are based on poststorm meteorological analyses from the National Hurricane Center (NHC). These analyses result in the creation of a “best track” database for each cyclone, consisting of 6-hourly representative estimates of the cyclone’s center location, maximum sustained (1-min average) surface (10 m) wind, and minimum sea level pressure (SLP). The best track identifies a system as a tropical cyclone at a particular time if NHC determines that it satisfies the following definition: “A warm-core, non-frontal synoptic-scale cyclone, originating over tropical or subtropical waters with organized deep convection and a closed surface wind circulation about a well-defined center” (NWS, cited 2009). The life

cycle of each cyclone (Table 1) is defined to include the tropical or subtropical depression stage, but does not include the remnant low or extratropical stages. The tracks for the season’s subtropical storms, tropical storms, and hurricanes, including their depression, extratropical, and remnant low stages (if applicable), are shown in Fig. 2.

Tools used for the analysis of Atlantic basin tropical cyclones include geostationary and low-earth orbiting satellites, aircraft reconnaissance, weather radar, buoys, and conventional land-based surface and upper-air observations (Dvorak 1984; Hebert and Poteat 1975; Hawkins et al. 2001; Brueske and Velden 2003; Demuth et al. 2006; Brennan et al. 2009). In 2007, during all NOAA WP-3D aircraft missions and a subset of the U.S. Air Force Reserve C-130 aircraft flights, surface winds were remotely estimated using the Stepped-Frequency Microwave Radiometer (SFMR) instrument (Uhlhorn et al. 2007). A more complete description of these datasets can be found in Franklin and Brown (2008).

In the cyclone summaries below, U.S. property damage estimates have been generally estimated by doubling the insured losses reported by the Property Claim Services of the Insurance Services Office; however, great uncertainty exists in estimating the cost of the damage caused by tropical cyclones. All damage amounts are reported in U.S. dollars unless otherwise indicated. Descriptions of the type and scope of damage are taken

TABLE 1. 2007 Atlantic hurricane season statistics.

No.	Name	Class ^a	Dates ^b	Max 1-min wind (kt)	Min SLP (mb)	Direct deaths	U.S. damage (\$ million)
1	Andrea	STS	9–11 May	50	1001	0	Minor ^c
2	Barry	TS	1–2 Jun	50	997	0	Minor ^c
3	Chantal	TS	31 Jul–1 Aug	45	994	0	0
4	Dean	MH	13–23 Aug	150	905	32	0
5	Erin	TS	15–19 Aug	35	1003	16	* ^d
6	Felix	MH	31 Aug–5 Sep	150	929	130	0
7	Gabrielle	TS	8–11 Sep	50	1004	0	Minor ^c
8	Humberto	H	12–14 Sep	80	985	1	50
9	Ingrid	TS	12–17 Sep	40	1002	40	0
10	Jerry	TS	23–24 Sep	35	1003	0	0
11	Karen	H	25–29 Sep	65	988	0	0
12	Lorenzo	H	25–28 Sep	70	990	6	0
13	Melissa	TS	28–30 Sep	35	1005	0	0
14	Noel	H	28 Oct–2 Nov	70	980	163	0
15	Olga	TS	11–12 Dec	50	1003	25	0

^a STS, subtropical storm with wind speeds of 34–63 kt ($17\text{--}32\text{ m s}^{-1}$); TS, tropical storm, with wind speeds of 34–63 kt ($17\text{--}32\text{ m s}^{-1}$); H, hurricane, with wind speeds of 64–95 kt ($33\text{--}49\text{ m s}^{-1}$); MH, major hurricane, hurricane with wind speeds of 96 kt (50 m s^{-1}) or higher.

^b Dates begin at 0000 UTC and include tropical and subtropical depression stages but exclude extratropical stage.

^c Only minor damage was reported, but the extent of the damage was not quantified.

^d A damage estimate for Erin was not provided by the Property Claim Services Division of the Insurance Services Office because the estimate did not surpass the threshold of \$25 million.

from local government officials, media reports, and local National Weather Service (NWS) Weather Forecast Offices (WFOs) in the affected areas. Tornado counts are based on reports provided by WFOs and/or the Storm Prediction Center. Tables of selected observations¹ are also provided for each cyclone. All dates and times are based on the coordinated universal time (UTC).

a. Subtropical Storm Andrea

Andrea formed from a large extratropical cyclone that originated just offshore of the U.S. mid-Atlantic coast on 6 May. The pre-Andrea cyclone deepened steadily, with the central pressure falling 16 mb (hPa) in the 24-h period ending at 0600 UTC 7 May. The cyclone initially was a mature extratropical cyclone, but by late on 7 May it lost most of its baroclinic support and development ended. However, interaction between the low and strong high pressure to the north produced a large area of hurricane-force winds, which in combination with the slow motion of the cyclone, generated large waves that impacted much of the coast of the southeastern United States and the Bahamas. On 8 May, the low weakened and began drifting westward over progressively warmer waters in the western Atlantic and deeper convection developed around the center as the vertical wind shear decreased. By early on 9 May, convection had become symmetric about the low-level center, the frontal and

cold-core structure had dissipated, and the wind field had contracted. As a result, the system became a subtropical cyclone by 0600 UTC 9 May while centered about 150 n mi east of Jacksonville, Florida.

The cyclone's weakening continued during the subtropical phase, so Andrea's peak intensity of 50 kt occurred at the time of subtropical cyclogenesis. Initially, Andrea drifted slowly westward within the retrograding middle- to upper-level cutoff low that had caused the pre-Andrea extratropical cyclogenesis. By late on 9 May, Andrea came under the influence of strong northerly flow aloft on the western side of the upper-level low, resulting in increasing vertical wind shear and a slow southward motion. The increase in vertical shear displaced the strongest convection southeast of the low-level center, and Andrea weakened to a depression by 1200 UTC 10 May while centered about 95 n mi east-southeast of Jacksonville. Lacking significant deep convection, Andrea degenerated into a remnant low by 0000 UTC 11 May. The remnants of Andrea produced intermittent bursts of deep convection on 11 May while drifting southward just offshore of the east-central coast of Florida. The remnant low accelerated northeastward on 12–13 May ahead of an advancing cold front and was absorbed into the front on 14 May.

Andrea's estimated peak intensity of 50 kt as a subtropical cyclone around 0600 UTC 9 May is based mainly on data from the National Aeronautics and Space Administration Quick Scatterometer (QuikSCAT). The peak wind of 65 kt during the extratropical phase is based on a maximum sustained wind of 55 kt with a gust to 70 kt reported at 0500 UTC 7 May by NOAA data buoy 41001,

¹ Additional observations for each cyclone can be found in NHC tropical cyclone reports (available online at <http://www.nhc.noaa.gov/2007atlan.shtml>).

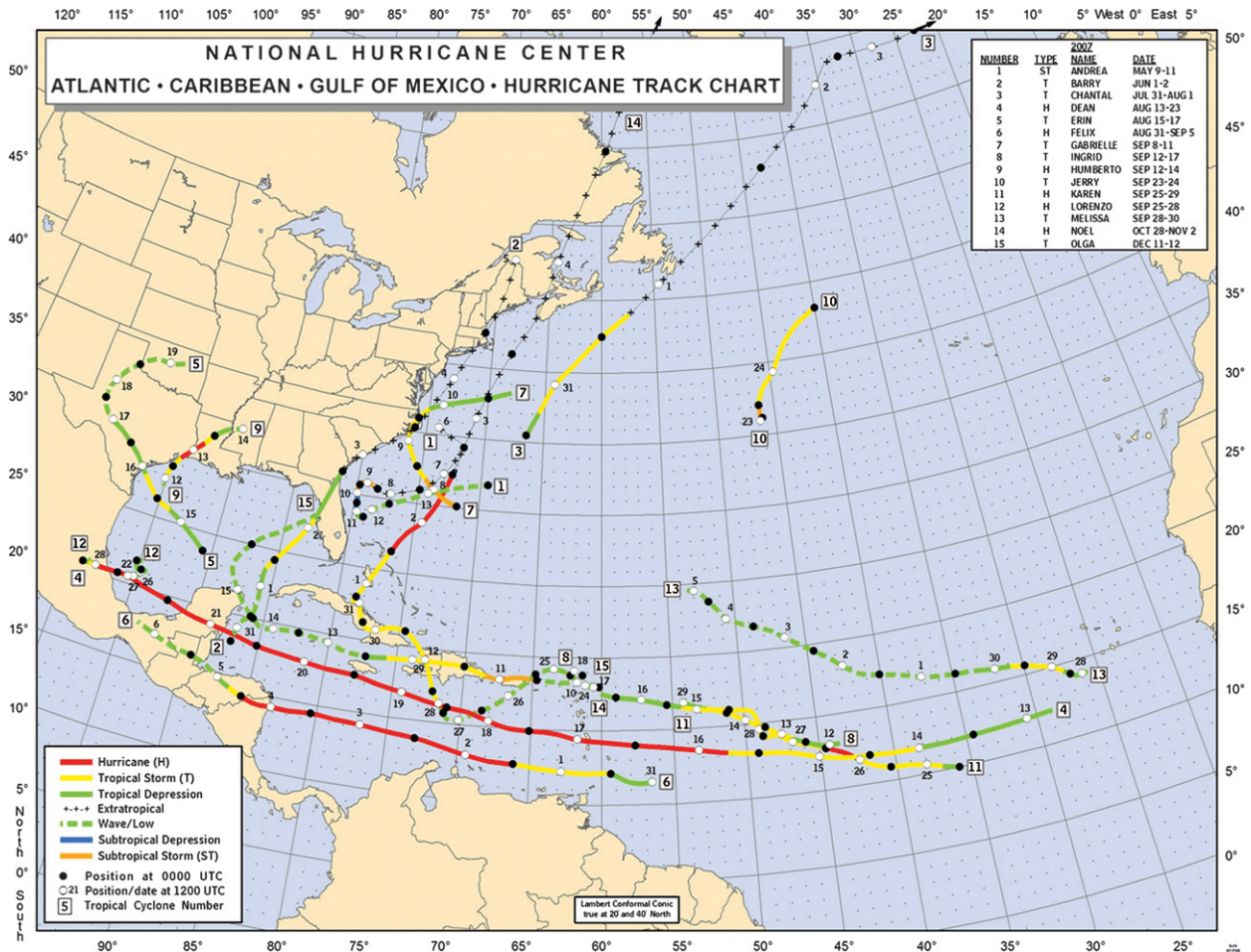


FIG. 2. Tracks of tropical storms, subtropical storms, and hurricanes in the Atlantic basin in 2007, including extratropical and remnant low stages.

which is located approximately 150 n mi east of Cape Hatteras.

There were no reports of deaths directly attributable to Andrea as a subtropical storm. However, the pre-Andrea extratropical cyclone was directly responsible for six deaths, including all four crew members of the 54-foot sailing vessel *Flying Colors*, whose last known location was off the coast of North Carolina on 7 May. Other fatalities were a kayaker who died after being pulled out to sea on 8 May near Seabrook Island, South Carolina, and a surfer who drowned after being overtaken by a large wave on 9 May near New Smyrna Beach, Florida.

Since Andrea never made landfall, most of the resulting damage was associated with the generation of large waves, higher than normal tides, and associated coastal flooding and beach erosion. Most of the significant damage occurred from North Carolina through Florida on 6–8 May as a result of very strong winds and waves associated with the pre-Andrea extratropical cy-

clone. A storm surge of 0.6–0.9 m was reported in St. Johns and Flagler Counties in northeastern Florida. Selected surface observations from land stations and data buoys from Andrea are given in Table 2.

b. Tropical Storm Barry

Barry formed from a westward-moving tropical wave that generated a broad area of low pressure near the eastern coast of the Yucatan Peninsula on 30 May. By 31 May, surface observations indicated that a circulation center had developed southeast of Cozumel, Mexico, but convection was disorganized and well removed from the area of low pressure. As the low moved north-northeastward over the northwestern Caribbean Sea and southeastern Gulf of Mexico, deep convection became somewhat concentrated near the center and a tropical depression formed just northwest of the western tip of Cuba at 1200 UTC 1 June.

TABLE 2. Selected surface observations for Subtropical Storm Andrea, 9–11 May (NOS is the National Ocean Service).

Location	Min SLP		Max surface wind speed			Storm surge (m) ^c	Storm tide (m) ^d	Total rain (mm)
	Time and date	Pressure (mb)	Time and date ^a	Sustained (kt) ^b	Gust (kt)			
Florida official								
Mayport Naval Base (KNRB)	2249 UTC 9 May	1007.8	1416 UTC 10 May		33			9.2
Jacksonville Beach (JAKF1)								19.6
Georgia official								
St. Simons Island (KSSI)	1608 UTC 9 May	1007.1	1458 UTC 10 May	35				1.8
Brunswick (BRUG1)								10.7
Woodbine (WBNG1)								14.5
Buoy/C-MAN/NOS								
Mayport, FL (MYPF1; 30.4°N, 81.4°W)	2230 UTC 9 May	1008.1	1400 UTC 10 May	24 ^e	33	0.76	1.91	
Fernandina Beach, FL (FRDF1; 30.7°N, 81.5°W)	2218 UTC 9 May	1007.3	2248 UTC 9 May	22 ^e	27	0.81	2.40	9.4
St. Simons Island NOS						0.86	0.86	

^a Date and time are for the sustained wind when both sustained and gust winds are listed.

^b Except as noted, sustained wind-averaging periods for C-MAN and land-based Automated Surface Observing System (ASOS) reports are 2 min; buoy-averaging periods are 8 min.

^c Storm surge is the water height above the normal astronomical tide level.

^d Storm tide is water height above the National Geodetic Vertical Datum (1929 mean sea level).

^e 6-min average wind.

The depression became a tropical storm at 1800 UTC that day while convection increased and the surface circulation became a little better organized. The cyclone reached its peak intensity of 50 kt, with a minimum pressure of 997 mb, at 0000 UTC 2 June, about 150 n mi west-southwest of the Dry Tortugas. Barry then weakened due to a mid- to upper-level trough over the central Gulf of Mexico that produced strong upper-level southwesterly winds over the cyclone. The center of Barry's broad circulation reached the Tampa Bay area around 1400 UTC 2 June, by which time the system had weakened to a tropical depression and begun to lose tropical characteristics. The depression moved between north-northeastward and northeastward across northern Florida and became extratropical by 0000 UTC 3 June over eastern Georgia. The extratropical cyclone intensified and moved toward the northeast along the east coast of the United States and was absorbed by a larger extratropical low around 1800 UTC 5 June near the St. Lawrence River.

While Barry's cloud pattern had features of both a tropical and a subtropical cyclone, data from the U.S. Air Force Reconnaissance plane during the afternoon of 1 June indicated that the area of strongest winds was within 5–10 n mi of the center, which is a structure more typical of tropical cyclones. Because of this structure and the development of organized convection near the center, Barry was classified as a tropical cyclone during this period.

Barry produced 200–300 mm of rainfall across the Cuban provinces of Pinar del Rio and Sancti Spiritus (Table 3). Barry also produced beneficial rains over

south Florida, with over 170 mm reported at West Palm Beach, and rainfall totals of 100–200 mm in eastern Georgia. Three tornadoes were reported in associated with Barry. One occurred in Playa Giron, Cuba, one in northern Sugarloaf Key in the Florida Keys, and one in Cutler Bay, Florida. The tornado that occurred on northern Sugarloaf Key produced moderate damage to roofing materials and the one in Cutler Bay produced roof damage to a home and uprooted large trees.

c. Tropical Storm Chantal

Chantal had its origins in a decaying frontal system that moved off the coast of the Carolinas on 21 July. A quasi-stationary area of disturbed weather formed a few hundred nautical miles east of the Bahamas by 26 July. Convection was intermittent over the area for the next few days while the system moved slowly northward. Very early on 31 July, a low-level circulation center developed with deep convection sufficiently organized to designate the system as a tropical depression about 210 n mi north-northwest of Bermuda. Over the next several hours, deep convection increased near the center, and the cyclone became a tropical storm. Surface wind retrievals from QuikSCAT indicate that Chantal reached a peak intensity of 45 kt later on 31 July.

A midtropospheric trough off the U.S. east coast forced Chantal northeastward with increasing forward speed. By early on 1 August, the circulation began to interact with a frontal zone, and Chantal began losing its tropical characteristics. The system became an

TABLE 3. Selected surface observations for Tropical Storm Barry, 1–2 Jun.

Location	Min SLP		Max surface wind speed		Storm surge (m) ^c	Storm tide (m) ^d	Total rain (mm)
	Time and date	Pressure (mb)	Time and date ^a	Sustained (kt) ^b			
Cuba							
Arroyo de Mantua, Pinar del Rio							280.4
Tope de Collantes, Sancti Spiritus (SS)							225.7
Caracusey, SS							305.3
Condado, SS							293.3
Florida official							
Key West (KEYW)			0522 UTC 2 Jun	34	41		
West Palm Beach (KPBI)							177.8
Georgia official							
Savannah Municipal Airport (KSAV)							132.5
Georgia unofficial							
Mount Vernon							203.5
Buoy/C-MAN/NOS							
Sombrero Key Light, FL (SMKF1; 24.6°N, 81.1°W)			0550 UTC 2 Jun	37	42		

^a Date and time are for the sustained wind when both the sustained and gust winds are listed.

^b Except as noted, sustained wind-averaging periods for C-MAN and land-based ASOS reports are 2 min; buoy-averaging periods are 10 min.

^c Storm surge is the water height above the normal astronomical tide level.

^d Storm tide is the water height above the National Geodetic Vertical Datum (1929 mean sea level).

extratropical cyclone later that day, and passed over the eastern end of the Avalon Peninsula of Newfoundland, producing heavy rainfall there. The extratropical remnants of Chantal intensified to near hurricane force on two separate occasions over the North Atlantic. Subsequently, the cyclone began weakening late on 3 August and passed a couple hundred nautical miles southeast of Iceland the next day. On 5 August, the system turned northeastward and lost its identity as it merged with another extratropical cyclone. No casualties or damage were reported in association with Chantal, but its extratropical remnants caused some flood-related damage in southeastern Newfoundland.

d. Hurricane Dean

1) SYNOPTIC HISTORY

Dean originated from a well-defined tropical wave that entered the Atlantic from the west coast of Africa on 11 August with a closed surface low center. Strong easterly shear kept the system's convection displaced from the elongated central area of light winds for a couple of days. By about 0600 UTC 13 August, a well-defined circulation center formed and became sufficiently connected to the deep convection to designate the low a tropical depression about 350 n mi west-southwest of Praia in the Cape Verde Islands.

The depression was embedded in strong, deep-layer easterly flow and initially moved westward at about 20 kt. The environment was still characterized by easterly shear, and the depression strengthened only slowly, reaching tropical storm strength around 1200 UTC 14 August, about 1250 n mi east of Barbados. Although the cyclone's satellite presentation remained ragged, it strengthened early the next day as it turned toward the west-northwest. Dean continued moving south of a deep-layer ridge for the next 7 days.

The easterly shear gradually abated, and by late on 15 August well-defined convective banding developed around the center and microwave data showed the formation of a partial eyewall. An eye appeared in infrared satellite imagery and Dean became a hurricane early on 16 August about 480 n mi east of Barbados. As upper-level outflow became more pronounced, Dean reached an intensity of 80 kt by 1200 UTC 16 August, but the eyewall then disappeared and the strengthening trend halted temporarily.

Dean entered the Caribbean Sea on 17 August, its center passing between Martinique and St. Lucia around 0930 UTC. The northern eyewall, accompanied by sustained winds of about 85 kt, passed directly over Martinique. With upper-level outflow increasing in all quadrants, Dean began to strengthen rapidly in the eastern Caribbean Sea, its winds increasing from 80 to

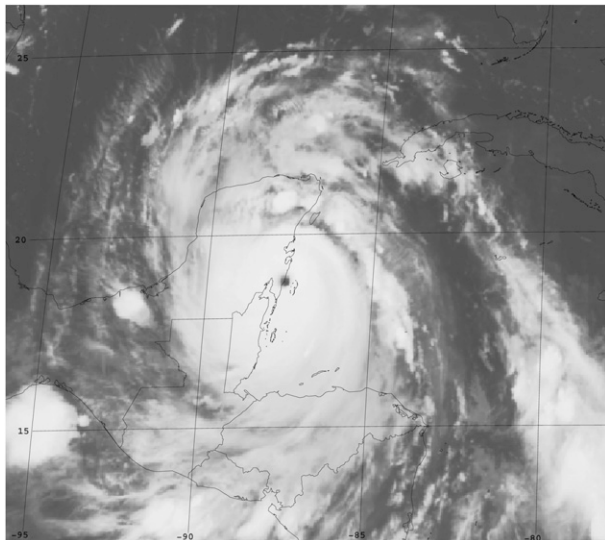


FIG. 3. GOES-12 IR satellite image of Hurricane Dean at 0815 UTC 21 Aug 2007, near the time of the cyclone's maximum intensity.

145 kt (from category 1 to category 5) in the 24 h ending at 0600 UTC 18 August. At 1200 UTC that day, Dean's minimum central pressure was 923 mb.

During this period of rapid deepening, Dean's forward motion slowed to about 15 kt as the center passed about 180 n mi south of Puerto Rico early on 18 August and continued west-northwestward toward Jamaica. By 1200 UTC that day, microwave imagery showed a concentric eyewall structure. As the inner eyewall eroded over the next 12 h, Dean's maximum sustained winds decreased from 145 to 120 kt (category 4). Interestingly, the central pressure fell slightly during this time, briefly dropping below 920 mb early on 19 August. Dean remained a category 4 hurricane while its center passed within about 80 n mi of the south coast of Haiti that morning. The center of Dean later passed within about 20 n mi of the south coast of Jamaica that evening with an intensity of 125 kt, although reconnaissance data suggest that Dean's strongest winds remained offshore.

On 20 August, Dean moved away from Jamaica over the deep warm waters of the northwestern Caribbean Sea. The convective structure that day was dominated by a single eyewall, and under light shear Dean began to strengthen as it approached the Yucatan Peninsula. When the eyewall contracted, Dean regained category 5 status around 0000 UTC 21 August and was still deepening when the center made landfall near Majahual in the Costa Maya tourist region of the Yucatan around 0830 UTC that day (Fig. 3). At the time of landfall, Dean is estimated to have had a minimum central pressure of 905 mb and maximum sustained winds of 150 kt, making

it the first landfalling category 5 hurricane in the Atlantic basin since Andrew (1992).

Dean weakened as it moved across the Yucatan Peninsula, and the cyclone emerged into the Bay of Campeche around 1900 UTC. Although Dean maintained hurricane strength over land, its inner-core convective structure was largely disrupted. Aircraft reconnaissance data in the Bay of Campeche showed that the cyclone's radius of maximum wind had expanded to roughly 55 n mi, and Dean was only able to reintensify slightly. A deep-layer ridge along the northern coast of the Gulf of Mexico kept Dean on a west-northwestward track until 1200 UTC 22 August, when the cyclone turned to the west. Dean made landfall as a category 2 hurricane with winds of 85 kt at 1630 UTC that day, its center passing near Tecolutla, Mexico, about 90 n mi northeast of Veracruz.

Dean weakened rapidly after landfall, becoming a depression by 0000 UTC 23 August and dissipating over the mountains of central Mexico shortly thereafter.

2) METEOROLOGICAL STATISTICS

There were a number of notable reconnaissance observations obtained during Dean, including an SFMR surface wind measurement of 150 kt at 0504 UTC 18 August. Examination of the SFMR wind profile across the eyewall reveals that Dean had a broad wind maximum, making it difficult to dismiss the SFMR maximum as unrepresentative, although the peak flight-level (700 mb) wind around this time was 154 kt, which would correspond to 139 kt at the surface using the standard 90% adjustment factor for this flight level. The best-track intensity for 0600 UTC 18 August of 145 kt represents a compromise between the SFMR and flight-level estimates.

The minimum pressure of Dean at the time of landfall as a category 5 hurricane on 21 August is estimated to be 905 mb, based on a dropsonde report of 906 mb at 0814 UTC with a surface wind speed of 15 kt. Dean had the third-lowest landfall pressure on record in the Atlantic basin, behind only Gilbert (1988) and the 1935 Labor Day hurricane.

The maximum winds at landfall are more difficult to estimate due to considerable spread among the observations around this time. The most extreme of these is a dropsonde surface report of 177 kt at 0728 UTC 21 August. This was associated with a very thin layer of strong winds immediately above the surface; consequently, this observation is rejected as unrepresentative of a sustained wind. Several hours prior to landfall, around 0000 UTC 21 August, there was good agreement between the SFMR and surface-adjusted flight-level winds on an intensity of 145 kt. Subsequently, the pressure fell from 914 to 905 mb, while the flight-level winds increased slightly. While the SFMR did not encounter

surface winds higher than 136 kt around the time of landfall, given the eyewall–convective structure, greater weight is placed on the flight-level observations, resulting in a landfall intensity estimate of 150 kt.

Selected surface observations from land stations are listed in Table 4. In Martinique, a sustained wind of 81 kt was observed at Vauclin outside of Dean's eyewall. A gust to 101 kt was reported at Sainte-Anne, which experienced the eyewall but has a more sheltered exposure. The highest storm-total rainfall in Martinique was 332.5 mm at Fort de France-Colson.

At Norman Manley International Airport in Kingston, Jamaica (MKJP), the weather station tower was blown over around 1800 UTC 19 August. Numerous rain gauges were blown or washed away. There was a ham radio report of an 89-kt sustained wind in Munro, St. Elizabeth, before the instrument failed. The highest rainfall report was 343 mm at Ingleside, Manchester.

No official wind observations of significance were received in association with Dean's landfalls in Mexico, which occurred in relatively sparsely populated areas. The maximum rainfall report was 391 mm at Requetemu, San Luis Potosi, in central mainland Mexico. In Sabancuy, Campeche, 276 mm of rain was recorded.

3) CASUALTY AND DAMAGE STATISTICS

The number of direct deaths associated with Dean is estimated to be 32, with 14 in Haiti, 12 in Mexico, 3 in Jamaica, 2 in Dominica, and 1 in St. Lucia. Remarkably, no deaths in Mexico occurred in association with the first landfall of Dean in that country. However, during Dean's second (weaker) landfall in Mexico, fatalities occurred in the states of Hidalgo, Puebla, Veracruz, and San Luis Potosi.

Flooding was reported throughout Martinique, where approximately 1300 homes were destroyed and another 7500 experienced severe damage. Media and government reports indicate severe losses to the banana and sugar cane crops. Damage has been estimated at €400 million. There were no direct deaths in Martinique, but there were at least three indirect deaths. Over 200 poststorm injuries were reported during the cleanup. In Guadeloupe, damage has been estimated at €100 million, with about 75% of the banana plantations destroyed.

Strong winds and heavy seas caused extensive damage to bridges, roofs, and utility poles along the north and west coasts of St. Lucia, where damage was estimated at \$18 million. In St. Vincent, some homes lost their roofs, and roof damage was also reported in Dominica. The banana crop in Dominica was completely lost. In Barbados, storm surge flooding was reported along the south coast.

The center of Dean passed about 90 n mi south of the Dominican Republic, where heavy surf along the south

coast destroyed several homes according to media reports. Landslides reportedly destroyed several hundred homes in Haiti and were responsible for most of the fatalities there.

In Jamaica, the most severe impacts were reported in the southeastern parishes of Clarendon, St. Catherine, and Kingston–St. Andrew, where it is estimated that roughly two-thirds of the homes were completely destroyed or required major repairs. Agriculture, particularly the banana crop, was severely impacted.

Dean made its initial landfall in Mexico in a relatively uninhabited area and consequently the damage was relatively light. Majahual was the only town to experience the full force of the hurricane, where hundreds of buildings were destroyed and steel girders were crumpled. Puerto Costa Maya, the nearby cruise port, was severely damaged and was expected to be closed for many months. The government of Belize reported damage of about \$100 million in that country. At Dean's second landfall near Tecalutla, Mexico, extensive roof damage was reported, along with downed trees and power lines.

e. Tropical Storm Erin

1) SYNOPTIC HISTORY

Erin formed in association with a tropical wave that entered the Atlantic from the west coast of Africa on 3 August and moved across the tropical Atlantic and eastern Caribbean Sea during the following week or so. A broad surface low formed in the western Caribbean in association with the wave on 12 August; however development was limited due to vertical wind shear south of an upper-level low centered over the eastern Gulf of Mexico. The upper-level low moved quickly westward during 13–14 August, allowing the vertical wind shear to decrease over the southeastern Gulf as the surface low moved into that area. Convection associated with the surface low increased and it is estimated that a tropical depression formed around 0000 UTC 15 August about 375 n mi east-southeast of Brownsville, Texas.

The depression moved northwestward to the south of a deep-layer ridge over the southern United States and became a tropical storm with maximum winds of 35 kt by 1800 UTC 15 August about 180 n mi east of Brownsville. Erin remained disorganized and failed to strengthen further over the Gulf, barely maintaining tropical storm status and making landfall on San Jose Island, Texas, on 16 August after it weakened to a 30-kt depression. The circulation remained intact as the system continued northwestward and inland, but Erin was no longer a tropical cyclone by 17 August as the convection became disorganized and intermittent when it

TABLE 4. Selected surface observations for Hurricane Dean, 13–23 Aug.

Location	Min SLP		Max surface wind speed			Storm surge (m) ^c	Storm tide (m) ^d	Total rain (mm)
	Time and date	Pressure (mb)	Time and date ^a	Sustained (kt) ^b	Gust (kt)			
Martinique								
Caravelle (elev: 38 m)			1000 UTC 17 Aug	68	78			
Diamant ^e (elev: 353 m)			0800 UTC 17 Aug	55	82			
Sainte-Anne ^e (elev: 13 m)			1100 UTC 17 Aug	66	101			
Vauclin ^e (elev: 19 m)			1100 UTC 17 Aug	81	93			
Lamentin airport (elev: 8 m)			1000 UTC 17 Aug	54	82			
Fort de France Desaix (elev: 140 m)			1100 UTC 17 Aug	73	99			
Fonds st Denis (elev: 510 m)			1100 UTC 17 Aug	73	113			
Fort de France Colson								332.5
Bellefontaine Verrier								304.5
Marin Usine								274.5
Sainte Anne Salines								260.5
Fort de France DDST								260.5
St. Lucia								
G. F. L. Charles Airport (TLPC)	1000 UTC 17 Aug	991.3		45	58			92.4
Hewanorra	0900 UTC 17 Aug	997.9	1000 UTC 17 Aug	38	58			53.4
Dominica								
Canefield Airport			1140 UTC 17 Aug		68			
Barbados								
Grantley Adams International Airport (78954)	0500 UTC 17 Aug	1004.2	0623 UTC 17 Aug	39	48			28.8
Dominican Republic								
Barahona (MDBH)			1200 UTC 19 Aug	45				
Jamaica								
Norman Manley International Airport	1930 UTC 19 Aug	991						130.5
Folly Point (Portland)	2058 UTC 19 Aug	1000	1928 UTC 19 Aug	44 ^f				106.1
Morant Point (St. Thomas)	2047 UTC 19 Aug	999.1	1747 UTC 19 Aug	54 ^f				
Ingleside, Manchester								343.4
Morant Bay, St. Thomas								332.0
Stony Hill, St. Andrew		992	2219 UTC 19 Aug	65				
Portmore, St. Catherine			2030 UTC 19 Aug	85				
Munro, St. Elizabeth			0000 UTC 20 Aug	89 ^e				
Lionel Town, Clarendon			2156 UTC 19 Aug	87				
Mexico								
Chetumal, Quintana Roo (MMCM)			1200 UTC 21 Aug	50	70			169.2
Isla Lobos, Veracruz			1730 UTC 22 Aug	44	57			62.8
Cayo Arcas, Campeche			0230 UTC 22 Aug	62	75			29.3
Tuxpan, Veracruz	1800 UTC 22 Aug	974.2						
Sabancuy, Campeche								276.5
Requetemu, San Luis Potosi								391.5

^a Date and time are for the sustained wind when both sustained and gust winds are listed.

^b Except as noted, the sustained wind-averaging periods for C-MAN and land-based ASOS reports are 2 min; buoy-averaging periods are 8 min.

^c Storm surge is the water height above the normal astronomical tide level.

^d Storm tide is the water height above the National Geodetic Vertical Datum (1929 mean sea level).

^e Record incomplete.

^f 10-min-average wind.

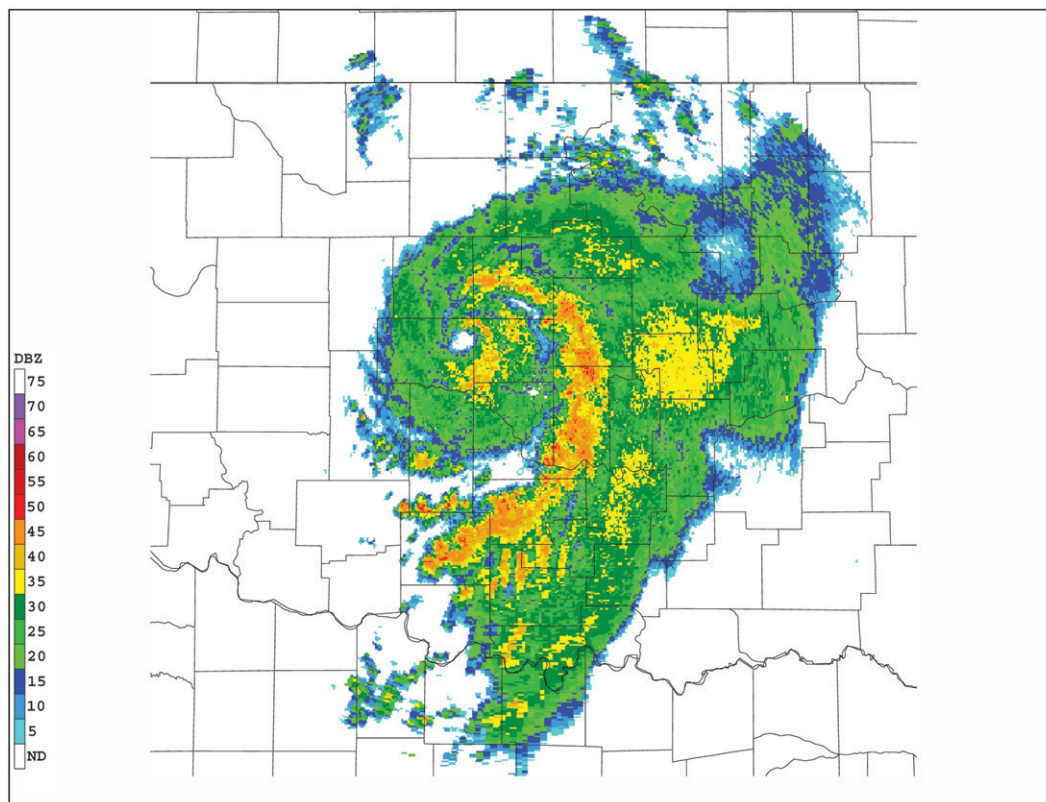


FIG. 4. Base reflectivity image from the Twin Lakes, OK, WSR-88D (KTLX) showing the remnants of Erin over central Oklahoma at 1201 UTC 19 Aug 2007.

was located about 50 n mi south of San Angelo, Texas. The low turned northward over extreme west Texas on 18 August as it moved around the western periphery of the ridge. Upon reaching the northwestern extent of the ridge, the low turned northeastward into southwestern Oklahoma very early on 19 August.

As the surface low moved east-northeastward across Oklahoma early on 19 August, associated thunderstorm activity abruptly increased when the low interacted with an eastward-moving upper-level short-wave trough. During an approximately 6-h period, sustained winds of gale force, with the highest reports around 50 kt, were observed at several locations in western and central Oklahoma. Isolated gusts of hurricane force, as high as 71 kt, were also observed. The system's organization briefly became dramatically enhanced, with an eyelike feature readily discernible in Weather Surveillance Radar-1988 Doppler (WSR-88D) imagery between about 0800 and 1300 UTC that day (Fig. 4). However, this episode was short lived and the eyelike feature quickly dissipated after 1300 UTC. The convective activity and strong winds had already begun to weaken by that time, as the upper-level short-wave trough moved eastward away from the surface low. The surface circulation dissipated shortly after

1800 UTC 19 August over northeastern Oklahoma, but remnant moisture continued northeastward into Missouri.

While the system's structure, particularly its convective organization as seen on radar, resembled a tropical or subtropical storm for a few hours on 19 August, the prevailing view from the National Hurricane Center's hurricane specialists is that the system was not a tropical or subtropical cyclone over Oklahoma. While this is a subjective determination, the deep convection is judged to have lasted an insufficient period of time to classify the system as a tropical or subtropical cyclone. It is speculated that the upper-level short-wave trough forced the deep convection to increase via upper-level diffluence while briefly superimposed above the surface low that provided a focus for low-level confluence. The upper-level forcing was apparently a dominant mechanism, but since the system was clearly nonfrontal over Oklahoma, designating it as an extratropical cyclone is not the most appropriate solution. Given all of these considerations, the system is simply designated as a "low" by NHC on 19 August.

2) METEOROLOGICAL STATISTICS

Erin's maximum intensity of 35 kt as a tropical cyclone is supported by aircraft reconnaissance data and

TABLE 5. Selected surface observations for Tropical Storm Erin, 15–19 Aug.

Location	Min SLP		Max surface wind speed			Storm surge (m) ^c	Storm tide (m) ^d	Total rain (mm)
	Time and date	Pressure (mb)	Time and date ^a	Sustained (kt) ^b	Gust (kt)			
Texas official								
Palacios (KPSX)								98.6
Pearland (KLVJ)								80.8
Wharton (KARM)								70.6
Houston-Bush Intercontinental Airport (KIAH)								65.8
Texas unofficial								
Jamaica Beach (western Galveston Island)	0859 UTC 16 Aug	1009.7	1523 UTC 16 Aug	26	34	0.94		
Hunting Bayou at Lockwood (Houston area)								245.1
Oklahoma official								
Watonga Regional Airport (KJWG)			0754 UTC 19 Aug	42	71			
7 mi W of Watonga (Mesonet WATO)	0725 UTC 19 Aug	999.1	0725 UTC 19 Aug	47	63			
4 mi NNW of Fort Cobb (Mesonet FTCB)	0525 UTC 19 Aug	1003.9	0525 UTC 19 Aug	43	65			236.2
Wiley Post Airport (Oklahoma City-Bethany, KPWA)	1153 UTC 19 Aug	1004.2	0919 UTC 19 Aug	39	49			
2 mi NE of Kingfisher (Mesonet KING)	1140 UTC 19 Aug	1004.2	0925 UTC 19 Aug	38	52			144.3
Will Rogers World Airport, Oklahoma City (KOKC)	1152 UTC 19 Aug	1006	0925 UTC 19 Aug	38	49			136.7
Guthrie-Edmond Regional Airport (KGOK)	1253 UTC 19 Aug	1006.6	0829 UTC 19 Aug	37	48			
El Reno Regional Airport (KRQO)			0741 UTC 19 Aug	37	48			
2 mi SSW of Minco (Mesonet MINC)	0720 UTC 19 Aug	1004.7	0815 UTC 19 Aug	37	50			172.7
7 mi W of Hinton (Mesonet HINT)	0800 UTC 19 Aug	1002.3	0625 UTC 19 Aug	37	56			
5 mi WNW of El Reno (Mesonet ELRE)	1050 UTC 19 Aug	1003.6	0745 UTC 19 Aug	37	47			214.6
3 mi W of Medicine Park (Mesonet MEDI)	0435 UTC 19 Aug	1002.4	0420 UTC 19 Aug	36	46			
4 mi WSW of Weatherford (Mesonet WEAT)	0630 UTC 19 Aug	1000.9	0505 UTC 19 Aug	36	48			165.9
Oklahoma unofficial								
9.8 mi NNW of Geary								281.7

^a Date and time are for the sustained wind when both the sustained and gust winds are listed.

^b Except as noted, the sustained wind-averaging periods for C-MAN and land-based ASOS reports are 2 min, the buoy-averaging periods are 8 min, and the wind-averaging period for OK Mesonet sites is 5 min.

^c Storm surge is the water height above the normal astronomical tide level.

^d Storm tide is the water height above the National Geodetic Vertical Datum (1929 mean sea level).

Dvorak estimates. The maximum intensity of the low over Oklahoma is set to 50 kt at 0600 UTC 19 August based on surface observations. Selected significant surface observations from land stations and data buoys are given in Table 5. An Oklahoma Mesonet site located 7 mi west of Watonga (about 50 n mi northwest of Oklahoma City) reported sustained winds (5-min average) of 47 kt near 0725 UTC, with sustained winds of gale force occurring there much of the time between

0600 and 0800 UTC. Nearby, a sustained wind of 42 kt, with a gust to 71 kt, was measured at Watonga Airport [an Automated Weather Observing System (AWOS) site] at 0754 UTC before the station ceased reporting. Several other observing sites east of the low center measured sustained winds of 35–40 kt at times from about 0500 UTC until almost 1200 UTC.

Erin and its remnants brought heavy rains to portions of southeastern, south-central, and western Texas; portions

of Oklahoma; and portions of southern Missouri. Storm-total rainfall amounts of 75–175 mm were common in these areas, with some locations receiving more than 250 mm (Table 5). Erin added to the effects of the flooding that had already occurred within the two prior weeks in the Nueces River basin south and west of San Antonio, Texas. Approximately 1 m of storm surge occurred in the Galveston area with Erin's landfall. A weak tornado was observed in the Houston area on 16 August. Following Erin's tropical cyclone phase, six tornadoes were reported in Oklahoma on 18–19 August.

3) CASUALTY AND DAMAGE STATISTICS

Erin directly caused nine fatalities in parts of southern and western Texas while the system was still a tropical cyclone. Thereafter, the remnants of Erin directly caused seven additional fatalities (six in Oklahoma, and one in Missouri). Most of the 16 total fatalities were due to inland flooding, including several deaths occurring when occupants drowned in automobiles swept away by floodwaters. On the day of landfall in the Houston area, several bayous reached flood stage, numerous roads were flooded, and more than 400 homes and 40 businesses were inundated. Minor beach erosion occurred in Galveston and Freeport, Texas. Significant damage occurred on 19 August in some communities northwest of Oklahoma City, where several homes were flooded, and strong winds damaged mobile homes and downed several trees and power lines. The Property Claim Services Division of the Insurance Services Office did not provide damage cost estimates for Erin because the damage amount did not surpass the threshold of \$25 million.

f. Hurricane Felix

1) SYNOPTIC OVERVIEW

Felix formed from a tropical wave that entered the Atlantic from Africa on 24 August. The wave moved westward for several days producing a persistent area of disorganized cloudiness and showers. On 29 August the showers became more organized and a tropical depression formed around 1200 UTC 31 August about 195 n mi east-southeast of Barbados.

The depression initially moved westward and became a tropical storm around 0000 UTC 1 September while centered about 60 n mi south of Barbados. The center of Felix passed over Grenada around 0845 UTC 1 September, then moved across the southern portion of the Caribbean Sea embedded in deep-layer easterly flow. Felix quickly strengthened, becoming a hurricane near 0000 UTC 2 September while centered about 155 n mi east of Bonaire in the Netherlands Antilles.

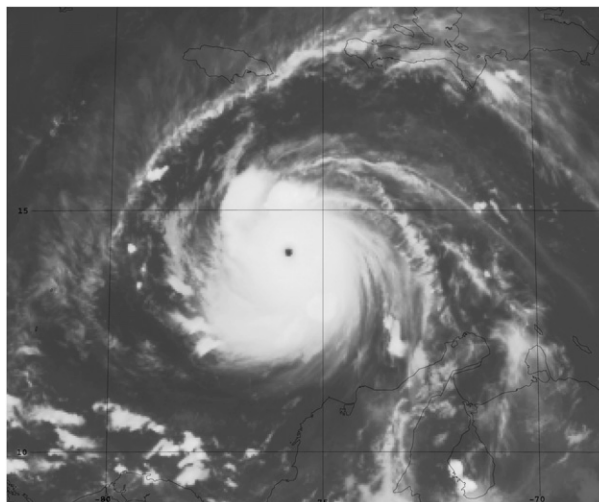


FIG. 5. GOES-12 IR satellite image of Hurricane Felix at 0815 UTC 3 Sep 2007, near the time of the cyclone's maximum intensity.

Felix moved just north of due west on 2 September, with its center passing 35–45 n mi north of the Netherlands Antilles. Rapid strengthening occurred during the day, with the maximum sustained winds increasing to 145 kt by 0000 UTC 3 September (category 5 on the Saffir–Simpson hurricane scale). The central pressure reached a minimum of 929 mb at 0700 UTC 3 September—a 64-mb fall in 32 h. Figure 5 shows a satellite image of Felix near the time of its peak intensity. An eyewall replacement cycle began later that day, and Felix weakened to a category 3 hurricane as the central pressure rose to 953 mb. Felix re-intensified at the end of the cycle and regained category 5 status just before landfall near Punta Gorda, Nicaragua, at 1200 UTC 4 September.

Felix weakened rapidly over northern Nicaragua and became a tropical storm less than 12 h after landfall. The cyclone decelerated and turned west-northwestward, and degenerated into a remnant low over northern Honduras early on 5 September. The low briefly moved over the Gulf of Honduras later that day, but no re-development occurred before it moved onshore in Belize and Guatemala. Although the remnant low dissipated over eastern Mexico late on 6 September, residual cloudiness and showers moved westward into the Pacific and could be tracked until 9 September.

2) METEOROLOGICAL STATISTICS

The first aircraft reconnaissance mission flown into Felix reported 42-kt winds at a flight level of 1500 ft at 2238 UTC 31 August, which is the basis for designating Felix as a tropical storm at 0000 UTC 1 September. These winds were found only a few nautical miles east of the center. Felix would remain a small hurricane

TABLE 6. Selected surface observations for Hurricane Felix, 31 Aug–5 Sep.

Location	Min SLP		Max surface wind speed			Storm surge (m) ^c	Storm tide (m) ^d	Total rain (mm)
	Time and date	Pressure (mb)	Time and date ^a	Sustained (kt) ^b	Gust (kt)			
Nicaragua Puerto Cabezas			1300 UTC 4 Sep	44				180.9
Honduras Omoa Cortes								244.7
Grenada Point Saline International Airport	0850 UTC 1 Sep	1001.0	0930 UTC 1 Sep		57			85.0
Barbados Grantley Adams International Airport	2000 UTC 31 Aug	1010.8	0230 UTC 1 Sep	30	43			21.6
Grenadine Islands Bequia	0656 UTC 1 Sep	1010.3	0801 UTC 1 Sep	26	47			25.4
St. Vincent E. T. Joshua Airport	0650 UTC 1 Sep	1011.1	0550 UTC 1 Sep	21	36			
Netherlands Antilles Aruba	1408 UTC 2 Sep	1008.4	1436 UTC 2 Sep	29 ^e	36			33.3
Bonaire	0727 UTC 2 Sep	1006.5	0636 UTC 2 Sep	25 ^e	31			22.4
Curacao	0922 UTC 2 Sep	1006.7	1052 UTC 2 Sep	20 ^e	28			54.4

^a Date and time are for the sustained wind when both the sustained and gust winds are listed.

^b Except as noted, the sustained wind-averaging periods are 10 min.

^c Storm surge is the water height above the normal astronomical tide level.

^d Storm tide is the water height above the National Geodetic Vertical Datum (1929 mean sea level).

^e 1-min average wind.

through its life, with tropical storm-force (hurricane force) winds never extending more than 100 n mi (40 n mi) from the center.

The intensity of Felix from 0000 to 0600 UTC 3 September has greater than normal uncertainty. The SFMR on board a NOAA Hurricane Hunter aircraft measured a 163-kt surface wind in the northeastern eyewall. However, the observed flight-level winds (152 kt at 700 mb), aircraft Doppler radar data, central pressure, and satellite signature do not support an intensity of 160–165 kt. Detailed data from the dropsonde suggest that the sonde and the SFMR both sampled a small-scale feature unrepresentative of the intensity of Felix at that time. As the plane passed through the southeastern eyewall, the SFMR estimated surface winds of 142 kt, while a dropsonde supported 130–140-kt surface sustained winds. Given the westward motion at the time, it is likely that stronger winds existed in the northern eyewall. The maximum intensity is conservatively set to 150 kt based on a blend of these data sources. During this eye penetration, the NOAA aircraft encountered turbulence and extreme vertical motions, forcing it to abort the mission and return to base.

Felix's winds increased by 115 kt, from 35 to 150 kt, in the 48-h period ending at 0000 UTC 3 September. In the 24-h period ending at that time, the winds increased by 85 kt. In the history of Atlantic tropical cyclones, only

Hurricane Wilma (2005) is known to have intensified more over 24- and 48-h periods.

The last flight into Felix before landfall in Nicaragua on 4 September found that the central pressure had fallen to 939 mb with 700-mb flight-level winds of 148 kt. The aircraft departed the storm about 5 h before landfall, and after its departure satellite imagery showed cooling of the eyewall cloud tops and warming of the eye. Objective Dvorak technique *T* numbers reached 6.9 (137 kt) at 1045 UTC, supporting category 5 intensity just before landfall.

Surface observations near the core of Felix were scarce (Table 6). Puerto Cabezas, Nicaragua reported sustained winds of 44 kt at 1300 UTC 4 September as the southern eyewall passed nearby. Point Saline International Airport on Grenada reported a wind gust of 57 kt at 0930 UTC 1 September and a minimum pressure of 1001.0 mb 40 min earlier. Bequia Island in the Grenadines reported a gust of 47 kt at 0606 UTC 1 September, while Barbados reported a gust of 43 kt at 0230 UTC that day. Aruba in the Netherlands Antilles reported a gust to 36 kt at 1436 UTC 2 September.

The small size and relatively fast movement of Felix resulted in relatively light rainfall totals along most of the track (Table 6). Heavier amounts occurred when the storm decelerated over Central America, with a maximum total of 244 mm at Omoa Cortes, Honduras.

3) CASUALTY AND DAMAGE STATISTICS

Media reports indicate that Felix caused 130 deaths in Nicaragua and Honduras, with 70 others missing. While the number killed in each country is not available, reports suggest that most of the deaths occurred in Nicaragua. Felix's landfall in Nicaragua caused severe damage to thousands of structures from winds and storm surge along the coast from Puerto Cabezas northward. Additional damage from rain-induced flooding occurred inland in both Nicaragua and Honduras. Monetary damage figures are not available. Wind and high surf caused minor damage on Aruba, Bonaire, and Curacao, while wind and lightning caused minor damage on St. Vincent and the Grenadines.

g. Tropical Storm Gabrielle

The genesis of Gabrielle can be traced to a low pressure area that formed along the coast of Georgia on 3 September. This low developed along a frontal boundary that moved off the southeastern coast of the United States on 1 September. After forming, the low moved eastward and remained nontropical for several days before becoming ill-defined on 5–6 September. The next day, a mid- to upper-level low formed several hundred miles southwest of Bermuda, moved slowly southwestward, and aided in the regeneration of the surface low over the western Atlantic. Satellite imagery suggests that the circulation became better defined later on 7 September, and a subtropical storm formed at 0000 UTC 8 September about 360 n mi southeast of Cape Hatteras, North Carolina.

Gabrielle transitioned to a tropical storm by 1800 UTC 8 September as convection developed just northwest of the center. The cyclone gradually strengthened while moving northwestward toward eastern North Carolina early on 9 September. Before Gabrielle reached the coast, reconnaissance aircraft data revealed that the center reformed closer to the convection, which was followed by some additional strengthening. Gabrielle reached a peak intensity of 50 kt at 1200 UTC 9 September, while centered just south-southeast of Cape Lookout, North Carolina. A few hours later, Gabrielle made landfall along the Cape Lookout National Seashore; however, strong northerly upper-level winds kept the convection and strongest surface winds offshore. Shortly after landfall, Gabrielle weakened due to the northerly wind shear and interaction with land. Gabrielle turned northeastward and exited the coast near Kill Devil Hills, North Carolina, just after 0000 UTC 10 September. After moving back over the Atlantic, convection continued to decrease near the center, and Gabrielle weakened to a tropical depression by 0600 UTC 10 September. The

depression moved east-northeastward, passing well southeast of the coast of the northeastern United States. The circulation of Gabrielle weakened and dissipated ahead of a frontal boundary by 1200 UTC 11 September about 300 n mi south-southwest of Nova Scotia.

The 50-kt peak intensity is based on a consensus of dropsonde data and the flight-level winds reduced to the surface using a standard reduction. These strong winds never reached the coast however, as northerly shear kept the most intense convection offshore for several hours. The highest sustained wind measured in eastern North Carolina was 38 kt at Frisco Pier (Table 7). A wind gust to 53 kt was observed at Ocracoke. Heavy rainfall was confined to a rather small area of eastern North Carolina, with a maximum of 229 mm reported near Harlowe in Carteret County. An estimated storm surge of 0.3–0.6 m occurred along the Atlantic-facing beaches of Carteret, Hyde, and Dare Counties, and a sound-side storm surge of 0.6–0.9 m was reported in portions of Dare County.

Impacts in eastern North Carolina were minimal and there were no reports of casualties. Storm surge and higher than normal tide levels contributed to overwash of North Carolina Highway 12 in Dare County, near Salvo and Rodanthe. A few streets in Morehead City and Beaufort were closed due to heavy rainfall and several homes and businesses suffered minor flood damage.

h. Hurricane Humberto

1) SYNOPTIC HISTORY

The genesis of Humberto can be traced to the remnants of the same frontal trough that was associated with the genesis of Gabrielle. After the trough moved over the southeastern Gulf of Mexico on 5 September, it remained nearly stationary for a couple of days, then moved slowly west-northwestward as high pressure built over the southeastern United States. On 11 September the trough was located over the northwestern Gulf of Mexico. Convection increased markedly near the trough axis that day a couple hundred nautical miles south of Galveston, Texas. Although thunderstorms diminished late on 11 September, a weak surface low had formed along the trough, and a tropical depression formed around 0900 UTC 12 September about 105 n mi south of Galveston when convection redeveloped near the low.

A ship report and WSR-88D data suggest that the depression quickly became a tropical storm around 1200 UTC 12 September as it moved slowly northward. Intense thunderstorms in well-defined spiral bands continued near the center as the small tropical cyclone continued to rapidly strengthen just offshore of the upper Texas coast. Later that day, the system turned to the north-northeast around a large midlevel ridge over the

TABLE 7. Selected surface observations for Tropical Storm Gabrielle, 8–11 Sep.

Location	Min SLP		Max surface wind speed			Storm surge (m) ^c	Storm tide (m) ^d	Total rain (mm)
	Time and date	Pressure (mb)	Time and date ^a	Sustained (kt) ^b	Gust (kt)			
North Carolina official								
Cape Hatteras (KHSE)	2015 UTC 9 Sep	1010.5	2341 UTC 9 Sep	34	46			5.9
Cedar Island (CITN7)	1550 UTC 9 Sep	1008.0						
Beaufort 6 N								211.2
North Carolina unofficial								
Avon Ocean (WeatherFlow)	1931 UTC 9 Sep	1009.0	1800 UTC 9 Sep	34	40			
Frisco Pier (WeatherFlow)	1928 UTC 9 Sep	1009.5	2330 UTC 9 Sep	38	45			
Frisco Woods (WeatherFlow)	1946 UTC 9 Sep	1009.5	2237 UTC 9 Sep	35	43			
Harlowe [7.2 mi ENE of Newport; Community Collaborative Rain, Hail and Snow (CoCoRaHS) network]								229.7
Morehead City								195.9
Ocracoke					53			
Ocracoke (WeatherFlow)	1803 UTC 9 Sep	1008.1	1711 UTC 9 Sep	37	43			
Buoy/C-MAN/NOS								
41025-Diamond Shoals (35.0°N, 75.4°W)	1950 UTC 9 Sep	1010.6	0120 UTC 10 Sep	36 ^e	45			

^a Date and time are for the sustained wind when both the sustained and gust winds are listed.

^b Except as noted, the sustained wind-averaging periods for C-MAN and land-based ASOS reports are 2 min; buoy-averaging periods are 8 min.

^c Storm surge is the water height above the normal astronomical tide level.

^d Storm tide is the water height above the National Geodetic Vertical Datum (1929 mean sea level).

^e 10-min average wind.

southeastern United States. WSR-88D data indicate that Humberto became a hurricane about 20 n mi south of High Island, Texas, around 0400 UTC 13 September, and the cyclone reached an estimated peak intensity of 80 kt as it made landfall just east of High Island in the McFaddin National Wildlife Refuge around 0700 UTC that day (Fig. 6). After landfall, the hurricane moved over extreme southeastern Texas across the Beaumont–Port Arthur area and into southwestern Louisiana. Humberto weakened to a tropical storm about 65 n mi west-northwest of Lafayette, Louisiana, and became a tropical depression near Alexandria, Louisiana, late on 13 September before dissipating the next day over central Mississippi.

2) METEOROLOGICAL STATISTICS

The genesis and rapid intensification of Humberto was remarkable. Around 0300 UTC 12 September, almost all convection associated with the cyclone's precursor surface low had dissipated, but by 0900 UTC that day convection became sufficiently organized for the system to be considered a tropical depression. A report of 38-kt winds from the ship *Tyco Decisive* and winds of 35–40 kt at an altitude of 7000–9000 ft from the Houston WSR-88D suggest that the depression became a tropical storm only 3 h later.

Humberto's landfall intensity of 80 kt is based on flight-level aircraft data and WSR-88D radar data. A

U.S. Air Force Reserve reconnaissance aircraft measured peak flight-level winds of 98 kt at 850 mb around the time of landfall, corresponding to about 78 kt at the surface. The SFMR measured surface winds of up to 85 kt just before landfall; however, the SFMR reading was taken in shallow waters where shoaling introduces measurement uncertainty. The peak winds from the

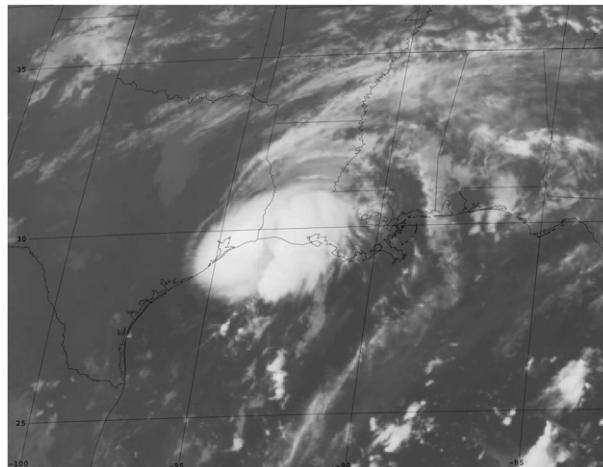


FIG. 6. GOES-12 IR satellite image of Hurricane Humberto at 0645 UTC 13 Sep 2007, near the time of the cyclone's maximum intensity.

TABLE 8. Selected surface observations for Hurricane Humberto, 12–14 Sep.

Location	Min SLP		Max surface wind speed			Storm surge (m) ^c	Storm tide (m) ^d	Total rain (mm)
	Time and date	Pressure (mb)	Time and date ^a	Sustained (kt) ^b	Gust (kt)			
Texas official								
McFaddin Wildlife Refuge RAWS (FADT2)			0735 UTC 13 Sep	52	65			
Southeast Texas Regional Airport (KBPT)	0927 UTC 13 Sep	988.5	0858 UTC 13 Sep	49	73			158.5
Beaumont (BEAT2)								167.4
Texas unofficial								
East Bay Bayou at Jones and Allen								359.5
Beaumont 2 SE								202.5
Beaumont Carroll State Park (TCEQ)			0900 UTC 13 Sep	33 ^f	65			
Beaumont Cathedral Christian School					46			
Beaumont KFDM-TV					43			
Beaumont Monsignor Kelly High School					49			
Beaumont Odom Academy					64			
Beaumont Richard Milburn Academy					55			
Beaumont St. Anne Catholic School					46			
Beaumont St. Anthony's Cathedral School					58			
Beaumont–Lamar (TCEQ)			0800 UTC 13 Sep		48 ^e			
Bolivar at Loop 108 (TXDOT)			0353 UTC 13 Sep	35	43			178.3
Eagle Point (TCOON)	0454 UTC 13 Sep	1007.8	0130 UTC 13 Sep		33	0.43	0.83	
Galveston Bay–North Jetty (TCOON)	0406 UTC 13 Sep	1003.4	0412 UTC 13 Sep	43 ^g	52	0.37	0.90	
Galveston Bay–Rollover Pass (TCOON)			0624 UTC 13 Sep	52 ^g	66	0.60	1.32	
Galveston Bay–South Jetty (TCOON)	0500 UTC 13 Sep	1003.4	0400 UTC 13 Sep	45 ^g	65		0.99	
GIWW at SH 124 Bridge								250.3
Golden Pass Ship Channel					101			
Hamshire (TCEQ)			0800 UTC 13 Sep	35 ^f	63 ^e			
Hamshire 5 SW								272.5
Jamaica Beach (JBHT2)	0214 UTC 13 Sep	1007.3	0047 UTC 13 Sep	30	35	0.77	1.04	147.6
Morgans Point (TCOON)						0.24	0.61	
Nederland High School (TCEQ)	0900 UTC 13 Sep	992.6	1000 UTC 13 Sep	25 ^f	60			
Port Arthur (TCOON)			0948 UTC 13 Sep	45 ^g	67	0.86	1.06	
Port Arthur 2 NNW	0909 UTC 13 Sep	989.4	0901 UTC 13 Sep	36				
Port Arthur City Service Center (TCEQ)			0800 UTC 13 Sep		70 ^e			
Port Arthur Lamar State College					65			
Port Arthur SETRPC (TCEQ)			0900 UTC 13 Sep	43 ^f	74 ^e			
Port Arthur West (TCEQ)			0900 UTC 13 Sep	34 ^f	67 ^e			
Rainbow Bridge						0.86	1.05	
Rollover Pass at Gilchrist (TXDOT)			0624 UTC 13 Sep	48	58			211.4
Texas Point (TCOON)	0906 UTC 13 Sep	1004.7	0924 UTC 13 Sep	40 ^g	54		1.48	
Louisiana official								
Lake Charles (KLCH)	1352 UTC 13 Sep	1009.5	0936 UTC 13 Sep	29	36			78.4
Alexandria–England AFB (KAEX)	2043 UTC 13 Sep	1005.4	1857 UTC 13 Sep	25	35			88.5

TABLE 8. (Continued)

Location	Min SLP		Max surface wind speed			Storm surge (m) ^c	Storm tide (m) ^d	Total rain (mm)
	Time and date	Pressure (mb)	Time and date ^a	Sustained (kt) ^b	Gust (kt)			
Louisiana unofficial								
De Ridder (DRIL1)								209.9
Cypremont Point						0.69	0.97	
Lake Charles						0.62	0.90	
Buoy/C-MAN/NOS								
Sabine Pass, TX (SRST2; 29.7°N, 94.1°W)	0800 UTC 13 Sep	997.0	0840 UTC 13 Sep	60 ^h	74			
42035-Galveston [22 n mi E of Galveston, TX (29.2°N, 94.4°W)]	0450 UTC 13 Sep	991.7	0410 UTC 13 Sep	50 ^h	64			
Galveston-Pleasure Pier (GPST2; 29.3°N, 94.8°W)	0406 UTC 13 Sep	1003.7	0336 UTC 13 Sep	43 ^g	56	0.86	1.10	
Sabine Pass North, TX (SBPT2; 29.7°N, 93.9°W)	0900 UTC 13 Sep	1003.3	0900 UTC 13 Sep	42 ^g	58	0.79	1.24	
Calcasieu Pass, LA (CAPL1; 29.8°N, 93.3°W)	1036 UTC 13 Sep	1009.4	0842 UTC 13 Sep	33 ^g	37	0.85	1.23	
Galveston Pier 21 (NOS)	0400 UTC 13 Sep	1005.1				0.47	0.93	129.2

^a Date and time are for the sustained wind when both the sustained and gust winds are listed.

^b Wind-averaging periods are 10 min.

^c Storm surge is the water height above the normal astronomical tide level.

^d Storm tide is the water height above the National Geodetic Vertical Datum (1929 mean sea level).

^e Instrument failed.

^f 5-min average wind.

^g 6-min average wind.

^h 10-min average wind.

Houston WSR-88D were about 100 kt at an elevation of around 3000 ft (915 m), and an approximate reduction factor of 75%–80% from that altitude suggests winds of 75–80 kt near the surface. Data from both the Houston and Lake Charles WSR-88Ds showed a deeper layer of 85–90-kt winds from 3000 to 9000 ft (915 to 2745 m), consistent with a near-surface wind estimate of about 75–80 kt.

The highest official near-surface wind reported was a 10-min-averaged sustained wind of 60 kt and gust to 74 kt from the Coastal-Marine Automated Network (C-MAN) station at Sea Rim State Park in Texas (Table 8). However, this station likely did not receive the maximum winds since radar data showed that the radius of maximum winds was several nautical miles to the west of the station. An unofficial wind gust measurement of 101 kt was received from a barge located in the Golden Pass ship channel near the Texas–Louisiana border. Based on surface and reconnaissance wind reports and radar estimates, sustained hurricane-force winds were likely observed in an area only about 15 n mi wide in extreme southwestern Louisiana and southeastern Texas. Humberto's 34-kt wind radii never exceeded 50 n mi.

The intensification rate in Humberto was one of the highest ever observed for an initially weak tropical cy-

clone. It is estimated that the cyclone strengthened from a 25-kt low into an 80-kt hurricane within 24 h. Only three other storms (Celia in 1970, and Arlene and Flora in 1963) have intensified more in 24 h from below tropical storm strength. While small cyclones are more likely to undergo rapid changes in intensity than large cyclones (e.g., DeMaria and Kaplan 1994), Humberto also had unusually well-defined banding and core convective structures in its formative stage, which likely provided the framework that allowed for the rapid development that occurred.

Very heavy rain occurred only in extreme southeastern Texas and southwestern Louisiana. The maximum storm total was 359 mm at East Bay Bayou, Texas, and a large surrounding area of 75–125-mm rainfall extended northeastward into central Louisiana. The highest storm tide was 1.48 m at the Texas Point gauge of the Texas Coastal Ocean Observation Network (TCOON). Storm surges of about 0.6–1.2 m were common from just east of Galveston Bay, Texas, eastward to near Lake Charles, Louisiana.

3) CASUALTY AND DAMAGE STATISTICS

There was one death directly associated with Humberto in Bridge City, Texas. Twelve injuries were reported in

southeastern Texas. Insured losses from Humberto are estimated by the Insurance Services Office to be less than \$50 million, and a rough estimate of the total property damage is about \$50 million. Most of the damage from Humberto was due to freshwater floods and strong winds, with the latter knocking down trees and power lines and causing roof damage.

i. Tropical Storm Ingrid

Ingrid developed from a large tropical wave early on 12 September about 980 n mi east of the Lesser Antilles. The depression moved generally west-northwestward within weak steering flow south of a midtropospheric ridge. Despite moderate westerly vertical wind shear, the cyclone became a tropical storm early on 13 September about 730 n mi east of the Lesser Antilles and reached its maximum intensity of 40 kt later that day. Persistent westerly shear caused Ingrid to weaken to a tropical depression on 15 September. Ingrid remained a depression for a day or so before degenerating into a remnant low early on 17 September, while centered about 140 n mi east-northeast of Antigua. The remnants of Ingrid moved slowly northwestward and west-northwestward until the low dissipated on 18 September. No damage or casualties from Ingrid were reported.

j. Tropical Storm Jerry

A nontropical low formed in the central North Atlantic on 21 September and meandered for a few days while gradually developing deep convection, which became better organized and eventually wrapped around the low. Since the system was still associated with an upper-level low and the strongest winds were well removed from the center, the depression that formed early on 23 September was subtropical. The cyclone still lacked a well-defined inner core when it strengthened into a subtropical storm later that day. Jerry evolved into a tropical storm with a peak intensity of 35 kt early on 24 September when deep convection developed near the center and the radius of maximum winds decreased. Thereafter, Jerry moved slowly toward the northeast over cooler waters and weakened. A strong cold front caused Jerry to accelerate northeastward, and early on 25 September the circulation dissipated ahead of the front. No damage or casualties from Jerry were reported.

k. Hurricane Karen

Karen formed from a tropical wave that moved off the west coast of Africa on 21 September. As the wave continued westward over the next couple of days, deep convection increased and a broad low-level circulation pattern gradually became better defined. The system moved west-northwestward with little change until late on

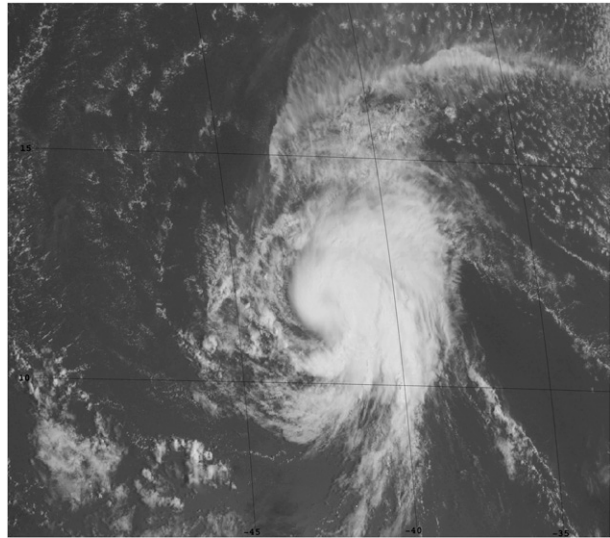


FIG. 7. GOES-12 visible satellite image of Hurricane Karen at 1215 UTC 26 Sep 2007, near the time of the cyclone's maximum intensity.

24 September, when convective banding became sufficient to signal the formation of a tropical depression about 720 n mi west-southwest of the Cape Verde Islands. The depression strengthened into a tropical storm a few hours later. After intensifying only slightly for about a day after its formation, Karen strengthened significantly early on 26 September, reaching hurricane strength and attaining its peak intensity of about 65 kt later that day (Fig. 7). Soon thereafter, a sharp upper-level trough west of the cyclone produced a substantial increase in southwesterly vertical wind shear. Karen quickly became disorganized and weakened below hurricane status early on 27 September. The shear caused the low-level circulation center to become exposed to the west and southwest of the deep convection, and Karen continued to weaken on 28 September, becoming a tropical depression by early on 29 September, when it turned westward in the low-level easterlies. The circulation dissipated later that day, although a remnant area of showers and squalls lingered near the Leeward Islands for a few more days.

A NOAA Hurricane Hunter mission measured peak 700-mb flight-level winds of 69 kt and SFMR surface winds of 62 kt shortly before 0000 UTC 27 September. These data support an intensity just below hurricane strength. However, by the time of the aircraft observations, Karen's appearance in satellite imagery was decidedly less organized than it had been 6–12 h earlier, when significantly better-defined banding features were seen. Moreover, a visible satellite image from around 1200 UTC 26 September showed a faint eyelike feature (Fig. 7). Therefore, it is estimated that Karen was a 65-kt hurricane at 1200 and 1800 UTC on 26 September, which

is consistent with Dvorak intensity estimates from NHC's Tropical Analysis and Forecast Branch (TAFB) at those times, which were based on the measurement of a banding feature that wrapped entirely around the center.

No casualties or damage from Karen were reported.

l. Hurricane Lorenzo

1) SYNOPTIC OVERVIEW

Lorenzo formed from a tropical wave that crossed the west coast of Africa on 11 September. On 21 September convection with the wave increased in the western Caribbean as the northern portion of the wave crossed the Yucatan Peninsula and entered the southern Gulf of Mexico. On 24 September, the wave spawned a small surface low in the southwestern Gulf, and convection increased. Strong upper-level winds initially inhibited development, but the upper-level flow began to relax the following day and a tropical depression formed around 1800 UTC 25 September about 150 n mi east-northeast of Tuxpan, Mexico. Steering currents were initially weak, and the depression made a small cyclonic loop during the next day or so. There was little development during this period due to upper-level southwesterly winds associated with a trough near the Texas coast. As the trough moved westward, however, the southwesterly upper-level flow gave way to an anticyclone, and the system became a tropical storm on 27 September about 130 n mi east of Tuxpan. Around this time, a midlevel ridge built eastward across the northern Gulf of Mexico and pushed Lorenzo toward the west. Lorenzo strengthened rapidly as it approached the coast, becoming a hurricane less than 12 h after reaching tropical storm intensity (Fig. 8). Lorenzo reached its peak intensity of 70 kt very early on 28 September and, then, weakened to 65 kt before landfall that morning near Tecolutla, Mexico. The small circulation weakened very rapidly over land, and the system decayed to a tropical depression and dissipated 18 h after landfall.

2) METEOROLOGICAL STATISTICS

Lorenzo may have reached hurricane strength a little earlier than indicated in the best track. The SFMR reported a maximum wind of 74 kt at 1917 UTC 27 September, and there was another series of SFMR observations of hurricane-force winds from 1731 to 1733 UTC to the southwest of the center. However, neither the central pressure (~1000 mb) nor the flight-level winds (64 kt at 1500 ft) supported hurricane intensity at this time. A peak intensity of 70 kt has been assigned at 0000 UTC 28 September, about the time that a closed eyewall became well defined on the Alvarado, Mexico, radar. The radar presentation of the center had degraded

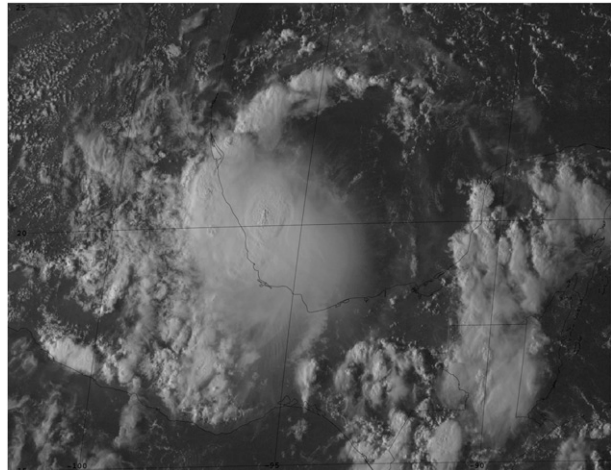


FIG. 8. GOES-12 visible satellite image of Hurricane Lorenzo at 2215 UTC 27 Sep 2007, about 2 h before the cyclone reached its maximum intensity.

by the time of landfall, and therefore an intensity of 65 kt is estimated at that time. At El Raudal in the state of Veracruz, 326.4 mm of rainfall was reported at and 301 mm was reported at Xicotepec in the state of Puebla.

3) CASUALTY AND DAMAGE STATISTICS

The government of Mexico reported six deaths attributable to Lorenzo: one in the state of Veracruz and five in Puebla. At least four of the deaths were caused by flash floods or mudslides. Damage in the two states included downed trees and power lines, as well as washed-out roads and flooded homes. Media reports indicate that high winds peeled off the roofs of homes in the seaside town of Nautla, south of where the center of Lorenzo made landfall. In Puebla, 169 homes were damaged and landslides made many roadways impassible. In the state of Hidalgo, flooding along the San Lorenzo River forced the evacuation of over 200 people.

m. Tropical Storm Melissa

Melissa originated from a tropical wave that entered the Atlantic from the west coast of Africa on 26 September and an area of low pressure formed the next day near the Cape Verde Islands. Convection with the low abruptly increased early on 28 September, and a tropical depression formed around 0600 UTC that day about 100 n mi west-southwest of the Cape Verde Islands. The depression was initially trapped in a region of very weak steering currents, as a deep-layer low pressure system over the northeastern Atlantic replaced the usual subtropical ridge. While moving very slowly westward, the cyclone strengthened slightly and became a tropical storm early on 29 September and remained at its peak intensity of 35 kt for the remainder of that day. Melissa

weakened to a depression early on 30 September in an environment of increasing westerly wind shear. As a shallower system, the cyclone began moving a little faster toward the west-northwest, to the south of a rebuilding low-level ridge. Convection decreased later that day and the depression degenerated into a remnant low about 475 n mi west of the Cape Verde Islands. Remaining south of the low-level ridge, the low continued generally west-northwestward for the next several days, producing intermittent convection until it dissipated within a frontal zone late on 5 October about 600 n mi northeast of the northern Leeward Islands. No casualties or damage were reported in association with Melissa.

n. Hurricane Noel

1) SYNOPTIC HISTORY

The tropical wave that played a role in the development of Noel entered the Atlantic from Africa early on 16 October. During the next several days, the wave moved westward without any signs of organization. As the wave approached the Lesser Antilles late on 22 October, it began to interact with a surface trough just north of the Leeward Islands and an upper-level trough that extended southwestward from the Atlantic into the eastern Caribbean Sea. A broad surface low pressure area formed about 150 n mi east-northeast of the northern Leeward Islands late on 23 October. The surface low moved slowly westward and produced disorganized thunderstorm activity over the next couple of days, while strong upper-level westerly winds inhibited further development. The low turned west-southwestward on 25 October, moving over the Virgin Islands and passing near the southeastern coast of Puerto Rico early the next day. On 27 October, the strong upper-level winds began to decrease, allowing convection to develop closer to the low center and the formation of a tropical depression about 185 n mi south-southeast of Port-Au-Prince, Haiti, by 0000 UTC 28 October.

The depression turned northwestward around the eastern side of a mid- to upper-level low located to the northwest of the tropical cyclone. Convection continued to increase and banding features became better defined during early on 28 October, and a 1200 UTC ship observation northeast of the center suggests that the depression had reached tropical storm strength by that time. Noel continued to strengthen, reaching an intensity of 50 kt 6 h later. As Noel continued moving northwestward toward the mountainous terrain along the southern coast of Haiti on 29 October, the low-level circulation was disrupted. Noel's maximum winds decreased to 45 kt before the center made landfall around

0700 UTC near Jacmel, about 20 n mi south-southwest of Port-Au-Prince.

The low-level circulation became very difficult to track as it passed along the west coast of Haiti. Visible satellite imagery suggested that a new low-level center formed near the northwestern coast of Haiti, shortly after 1200 UTC 29 October, and a reconnaissance mission later that afternoon reported wind and pressure data consistent with the satellite position estimate.

The mid- to upper-level low that had been steering Noel northwestward weakened late on 29 October and the cyclone turned westward to the south of a midlevel ridge over the western Atlantic. During this time, Noel hugged the northern coast of eastern Cuba and regained an intensity of 50 kt. Surface data and radar observations from Holguin, Cuba, indicate the center of Noel passed near or just north of Cabo Lucrecia and made landfall around 0600 UTC near Guardalavaca, Cuba. A few hours later, the center passed near La Jiquima, where a minimum pressure of 997.9 mb was recorded. While Noel's center was over the island for a little more than 30 h, maximum winds decreased, but ship and surface observations show that Noel remained a minimal tropical storm. For the first 18 h over Cuba, Noel moved a little to the south of due west, then turned northwestward and north-northwestward and reemerged over the Atlantic waters along the north-central coast of Cuba near Cayo Coco, shortly after 1200 UTC 31 October.

Once over water, the tropical storm regained strength and meandered just north of Cuba as the low-level center was displaced to the southwest of the convection due to southwesterly wind shear. Early on 1 November, Noel turned north-northeastward ahead of a midlatitude trough moving across the Gulf of Mexico and a very strong burst of deep convection developed just northeast of the center. Noel had maximum winds of 50 kt as the center moved across Andros Island in the northwest Bahamas shortly after 1200 UTC that day. Six hours later, the cyclone intensified to 55 kt as its center passed very near Nassau. Despite the southwesterly shear, Noel continued to intensify, and the cyclone attained hurricane strength shortly after passing between Eleuthera and Abaco Islands. Noel reached a peak intensity of 70 kt around 0000 UTC 2 November and accelerated north-eastward ahead of the midlatitude trough (Fig. 9). Shortly thereafter, the satellite appearance of Noel began to deteriorate as the inner-core convection weakened. By 0000 UTC 3 November, Noel lacked the deep convection required of a tropical cyclone and became extratropical, centered about 240 n mi southeast of Cape Hatteras, North Carolina.

The extratropical remnant of Noel became a very large and powerful cyclone as it moved north-northeastward



FIG. 9. GOES-12 visible satellite image of Hurricane Noel at 0015 UTC 2 Nov 2007, near the time of the cyclone's maximum intensity.

off the east coast of the United States, reaching a peak intensity of 75 kt at 1200 UTC 3 November before weakening slightly late that day as it passed about 75 n mi east-southeast of Nantucket Island, Massachusetts. Shortly after 0600 UTC 4 November, the cyclone made landfall near Chebogue Point, Nova Scotia, with maximum winds of 65 kt. The cyclone weakened over eastern Canada and exited the coast of Labrador about 18 h later. The low continued northeastward and merged with another extratropical cyclone over Greenland by 0600 UTC 6 November.

2) METEOROLOGICAL STATISTICS

The highest wind gust recorded on the island of Hispaniola was 60 kt at Barahona, Dominican Republic, at 0815 UTC 29 October. Most official observing sites in eastern Cuba reported maximum wind gusts between 30 and 40 kt (Table 9).

The 70-kt peak intensity of Noel is based on several SFMR surface wind estimates on 2 November. A maximum flight-level wind of 89 kt was observed at 0216 UTC 2 November, which would typically correspond to an 80-kt surface wind using the standard 90% adjustment. However, SFMR and dropwindsonde data at this time suggest that the standard 90% adjustment was likely not valid. The highest SFMR wind during the mission was 70 kt and a dropwindsonde at 0520 UTC provided a surface wind estimate of 70 kt (derived from the lowest 150 m). A subsequent reconnaissance mission between 1200 and 1800 UTC 2 November recorded a maximum flight-level wind of 90 kt at 700 mb, but again the highest surface wind estimate from the SFMR during this flight was 70 kt. The 75-kt peak intensity of the extratropical

cyclone is based on QuikSCAT data from 1024 UTC 3 November.

Reconnaissance data early on 3 November suggest that Noel maintained a residual shallow warm core at the time the cyclone was classified as extratropical. Despite this, the significant decrease in inner-core convection after 1200 UTC 2 November meant that Noel no longer satisfied the convective requirement to be a tropical cyclone by 0000 UTC 3 November.

Noel produced several days of torrential rainfall across Hispaniola and Cuba. The maximum rainfall reported from Haiti was 654.8 mm from Camp Perrin, located near Cayes along the southwestern coast, which is a 5-day total ending at 0600 local time 2 November. Rainfall reports received from the Dominican Republic include accumulations from 25 to 31 October, a period that includes the precursor low of Noel; the heaviest rains fell between 28 and 31 October. Several locations in the Dominican Republic reported totals between 380 and 635 mm, with a maximum of 905 mm at Angelina. However, the rainfall totals from several of these locations are incomplete, as the gauges exceeded their maximum capacity, in some cases on several consecutive days. At Angelina, the rain gauge reached its capacity of 300 mm on two consecutive days, while at Rancho Arriba (total rainfall 812 mm) the rain gauge reached its capacity of 170 mm on four consecutive days (28–31 October). It is possible that the maximum rainfall in the Dominican Republic from Noel and its precursor disturbance may have approached 1000 mm.

Rainfall accumulations of 125–300 mm were common across eastern Cuba. In the province of Holguin, 310 mm fell at Loynaz Hechavarria during the 24-h period ending at 1200 UTC 31 October. In the Bahamas, 748 mm of rain fell on Long Island during the 79-h period between 0200 UTC 30 October and 0900 UTC 2 November. The precursor low also produced significant rainfall across Puerto Rico and the Virgin Islands, with a maximum of 438 mm at Gate Tower, Puerto Rico.

The combination of Noel over the northern Caribbean and strong high pressure over the eastern United States produced a strong pressure gradient over the western Atlantic and Florida between 29 and 31 October, resulting in an extended period of gale-force winds along the east coast of Florida that were not directly associated with the circulation of Noel. The extratropical remnant of Noel produced very strong winds along coastal sections of the United States from the Carolinas northward as it passed offshore. The strongest winds were observed in eastern Massachusetts, where a sustained wind of 51 kt and a 63-kt gust were measured on Nantucket Island and a gust to 77 kt was observed at Barnstable, Massachusetts. In eastern Maine, wind gusts as high as 57 kt were recorded. In eastern Canada, hurricane-force

TABLE 9. (Continued)

Location	Min SLP		Max surface wind speed			Storm surge (m) ^c	Storm tide (m) ^d	Total rain (mm)
	Time and date	Pressure (mb)	Time and date ^a	Sustained (kt) ^b	Gust (kt)			
Long Island Rock Sound (78080) (Eleuthera)	2000 UTC 1 Nov	994.3	1900 UTC 1 Nov	35				748.7
Buoy/C-MAN/NOS 41047-NE of Bahamas (27.5°N, 71.5°W)	1211 UTC 2 Nov	1001.0	1353 UTC 2 Nov	54 ⁱ	62			

^a Date and time are for the sustained wind when both sustained and gust winds are listed.

^b Except as noted, sustained wind-averaging periods for C-MAN and land-based ASOS reports are 2 min; buoy-averaging periods are 8 min.

^c Storm surge is the water height above the normal astronomical tide level.

^d Storm tide is the water height above the National Geodetic Vertical Datum (1929 MSL).

^e Rainfall totals from the Dominican Republic are accumulations between 25 and 31 October. The totals include rainfall from Noel and its precursor low.

^f Incomplete.

^g Rainfall totals from Haiti are accumulations between 28 and 30 October.

^h Elevated location.

ⁱ 1-min average wind.

wind gusts occurred in portions of Nova Scotia and Newfoundland. The highest sustained wind was 61 kt at McNab's Island in Halifax Harbor, with maximum gusts of 97 kt at Wreckhouse, Newfoundland, and 79 kt at Grand Etang, Nova Scotia. The extratropical cyclone produced a wide swath of 50–100 mm of precipitation from coastal sections of Massachusetts northward across Maine, Nova Scotia, New Brunswick, and eastern Quebec, including significant snowfall in some areas. The highest precipitation total in the United States was 128 mm at Cutler Rainwise, Maine, and the highest in Canada was 134 mm at Cap D'Espoir in southeastern Quebec.

3) CASUALTY AND DAMAGE STATISTICS

Rains from Noel produced widespread damage and loss of life in the Dominican Republic, Haiti, Jamaica, eastern Cuba, and the Bahamas. Noel is estimated to have caused a total of 163 deaths, with 59 others missing. On 16 November 2007, the United Nations Office for the Coordination of Humanitarian Affairs listed the death toll in the Dominican Republic at 87, with 42 people missing. The exact number of deaths in Haiti has been somewhat difficult to determine, as counts have ranged from 57 to 103. This report uses the count of 73 fatalities from the Haitian Direction of the Civil Protection, which appears to include only the deaths directly attributed to the tropical cyclone. Reports indicate that Noel was responsible for one death in the Bahamas, one in Jamaica, and one in Cuba. Nearly all of these fatalities were the result of floods and mudslides.

Reports indicate that Noel is estimated to have damaged nearly 15 000 homes with around 6000 homes

destroyed in the Dominican Republic, displacing as many as 78 000 people. Mudslides and floods washed away several bridges that left numerous towns and villages isolated for many days. The government of the Dominican Republic reported that crop losses totaled \$77.7 million. In Haiti, the government reported that nearly 18 000 homes were damaged and almost 4000 homes were destroyed, while numerous crops were ruined by floods.

The Reuters news service reported that 80 000 residents in Cuba were evacuated from Noel's flooding. Twenty-two thousand houses were damaged or destroyed along with over 8000 mi (13 000 km) of roads. Agricultural losses accounted for \$305 million of the \$500 million in financial losses in Cuba as reported by the Granma International Newspaper on 8 November 2007. Officials reported that Cuba lost 10% of its coffee crop and that nearly 125 000 acres of sugar cane fields were flooded or damaged. Damage to homes amounted to \$128 million, with an estimated \$33 million in damage to power and communication lines. The Cuban Meteorological Service stated that rains from Noel produced the worst flooding since Hurricane Flora (1963).

Media reports from the Bahamas indicate that severe flooding occurred on Cat Island, Exuma, and Long Island, with water inundating several homes. One drowning death occurred in Exuma.

The extratropical remnant of Noel produced strong winds that downed trees and power lines in the northeastern United States and eastern Canada. Media reports indicate that 190 000 homes and businesses in eastern Canada and about 80 000 homes in the northeastern United States lost power. Coastal floods and significant

wave action washed out sections of coastal roads in Nova Scotia, damaging several waterfront buildings.

Gale-force winds created by the combination of Noel and a strong high over the eastern United States generated very large waves that pounded the east coast of Florida for several days, producing significant beach erosion prior to Noel's center passing offshore. Additional beach erosion was reported along the Atlantic coast from the Carolinas northward.

o. Tropical Storm Olga

Although quite rare, Olga's formation marks the eighth time a named storm has formed in the Atlantic basin during December in the reconnaissance era (since 1944). Olga formed from the interaction between an upper-level low and a low-level trough over the central Atlantic Ocean. Early on 6 December, a broad upper-level low developed over the east-central Atlantic along with an associated low-level trough that stretched along 35°W between 20° and 30°N. These features moved uneventfully westward at 15–20 kt during the next couple of days. Late on 8 December, convection developed in the vicinity of the upper-level low and surface trough. By 10 December, a broad area of surface low pressure formed about 350 n mi east of Puerto Rico. Although convection remained disorganized at that time, the low produced gale-force winds north of its center. Early on 11 December, the system developed a well-defined surface circulation and convection relatively close to the center and was designated a subtropical storm about 50 n mi east of San Juan, Puerto Rico.

Under the influence of a low- to midlevel ridge to its north, Olga moved westward along the northern coast of Puerto Rico and made landfall along the north-central coast of the island early on 11 December. Convection increased near the center and the radius of maximum winds decreased; late on 11 December Olga became a tropical storm at its peak intensity of 50 kt as it made landfall just south of Punta Cana in the Dominican Republic. Despite the mountainous terrain, Olga maintained its peak intensity for about 12 h while moving across eastern Hispaniola; however, the strongest winds remained offshore with the deepest convection. Olga finally weakened over central Hispaniola, and when it emerged over the Windward Passage on 12 December, the intensity had decreased to 35 kt. Olga became a tropical depression later that day and degenerated into a remnant low the next day north of Jamaica.

The remnant low continued westward across the northwestern Caribbean Sea during the next couple of days. By 15 December, the low moved northwestward and northward around the western periphery of a low- to midlevel ridge. Later that day and early on 16 December, the rem-

nants of Olga accelerated northeastward over the eastern Gulf of Mexico ahead of an approaching cold front, producing disorganized thunderstorms. Satellite imagery and radar data suggest that, later on 16 December, a small circulation crossed the west-central coast of Florida, just north of Tampa, and was quickly absorbed into the cold front.

The primary impact of Olga was heavy rainfall in portions of Puerto Rico and Hispaniola. Maximum rainfall totals ranged from around 280 mm in central Puerto Rico to over 380 mm in the Dominican Republic (Table 10). As the remnants of Olga interacted with the cold front and prefrontal squall line, sustained winds of tropical-storm force with gusts to hurricane force were produced in Clearwater Beach, Florida.

At least 22 deaths were attributed to Olga in the Dominican Republic according to the Dominican Republic Meteorological Office, primarily due to torrential rainfall, mudslides, and flooding of the Yaque River. In addition, two deaths in Haiti and one death in Puerto Rico were reported. The impact of the cyclone was enhanced due to the ground being already saturated from the passage of then-Tropical Storm Noel at the end of October. News reports indicate that almost 12 000 homes were damaged, including 370 that were completely destroyed, causing more than 60 000 people to be displaced. When Olga's remnants moved rapidly across Florida, a tornado touched down in central Florida in Pasco County, causing damage to several buildings.

3. Nondeveloping tropical depressions

Two tropical depressions developed during the 2007 season that did not reach tropical storm strength. Tropical Depression 10 developed from the complex interaction between an upper-level low, a decaying frontal zone, and a tropical wave. The tropical wave reached the Bahamas on 17 September and produced an area of disorganized showers and thunderstorms. At the same time, a cold front pushed southward over the eastern United States and became stationary over central Florida and the western Atlantic. The stationary front produced a large area of showers and thunderstorms that extended from northern Florida northeastward over the western Atlantic for several hundred nautical miles. The areas of convection associated with the tropical wave and weakening stationary front merged on 18 September as a large upper-level low formed over Florida, producing a broad area of surface low pressure over the northwestern Bahamas. The surface low deepened over the next 24 h as it moved westward over central Florida.

The broad surface low contained multiple embedded vorticity centers as it emerged into the eastern Gulf of

TABLE 10. Selected surface observations for Tropical Storm Olga, 11–12 Dec.

Location	Min SLP		Max surface wind speed			Storm surge (m) ^c	Storm tide (m) ^d	Total rain (mm)
	Time and date	Pressure (mb)	Time and date ^a	Sustained (kt) ^b	Gust (kt)			
Dominican Republic ^e								
Catey airport			2300 UTC 11 Dec		55			118.3
Jarabacoa								226.9 ^f
Polo								389.7
Puerto Plata (78458)	0300 UTC 12 Dec	1010.0	0300 UTC 12 Dec		35			
Punta Cana (78479)	1300 UTC 11 Dec	1003.0	1300 UTC 11 Dec	35				143.7
Rancho Arriba								255.7 ^f
Puerto Rico and Virgin Islands								
Cyril E. King Airport (St. Thomas, TIST)			1153 UTC 10 Dec		42			
San Juan airport (TJSJ)			0426 UTC 11 Dec		32			
Ponce, Rio Cerrillos above Lago Cerrillos								283.2
Villalba								242.7
Bahamas								
Turks Island (78118)			0316 UTC 12 Dec	34				
Buoy/C-MAN/NOS								
41043-southwestern Atlantic (21.0°N, 65.1°W)	0350 UTC 11 Dec	1012.3	0616 UTC 12 Dec	37 ^g	49			

^a Date and time are for sustained winds when both sustained and gust winds are listed.

^b Except as noted, sustained wind-averaging periods for C-MAN and land-based ASOS reports are 2 min; buoy-averaging periods are 8 min.

^c Storm surge is the water height above the normal astronomical tide level.

^d Storm tide is the water height above the National Geodetic Vertical Datum (1929 mean sea level).

^e Rainfall totals from the Dominican Republic are accumulations between 11 and 12 December. All information is received from the Dominican Republic Meteorological Office.

^f Incomplete.

^g 1-min average wind.

Mexico, but one of these centers became dominant around 1200 UTC 21 September about 40 n mi southwest of Apalachicola, Florida. Given the system's association with the upper-level low, the cyclone was initially classified as a subtropical depression. The depression quickly acquired tropical characteristics as it separated from the upper low and its convection increased near the low-level center during the afternoon of 21 September. The depression continued west-northwestward with little development and made landfall near Fort Walton Beach, Florida, around 0000 UTC 22 September. Shortly after landfall, the depression degenerated into a remnant low that continued northward and dissipated over southwestern Alabama shortly after 0600 UTC 22 September. The depression's precursor produced two tornadoes on 20 September: one near Eustis, Florida, that destroyed several homes in the area, and a second near Mayo, Florida, which caused minor damage. Otherwise, the impacts were minimal.

Tropical Depression 15 formed from a large area of disturbed weather that extended from the northwestern Caribbean through the Bahamas. A broad area of low pressure developed on 8 October about 130 n mi north-

east of the Turks and Caicos Islands. The low moved east-northeastward and a tropical depression formed about 645 n mi east-southeast of Bermuda on 11 October. As the depression turned eastward and slowed, an upper-level trough moved over the depression and strong northerly wind shear developed. Because of the shear, the depression lost all of its deep convection and degenerated into a remnant low about 790 n mi east of Bermuda on 12 October. The remnant low moved northwestward on 13 October, then turned northeastward and merged with a frontal zone on 14 October. The resulting extratropical low developed gale-force winds on 16 October until it was absorbed by a larger extratropical low on 17 October north of the Azores.

4. Forecast verification and warnings

For all operationally designated tropical (or subtropical) cyclones in the Atlantic and eastern North Pacific basins, NHC issues an "official" forecast of the cyclone's center location and maximum 1-min surface wind speed. Forecasts are issued every 6 h and contain projections valid 12, 24, 36, 48, 72, 96, and 120 h after

TABLE 11. Homogenous comparison of official and CLIPER5 track forecast errors in the Atlantic basin for the 2007 season for all tropical and subtropical cyclones. Long-term averages are shown for comparison.

	Forecast period (h)						
	12	24	36	48	72	96	120
2007 avg official error (n mi)	33	51	71	92	146	167	258
2007 avg CLIPER5 error (n mi)	45	85	122	160	237	323	512
2007 avg error relative to CLIPER5 (%)	-28	-40	-42	-43	-38	-48	-50
2007 avg official bias vector ($^{\circ}$ /n mi $^{-1}$)	341/3	001/7	026/17	035/34	046/75	059/107	069/162
2007 No. of cases	177	145	116	93	62	39	23
2002-06 avg official error (n mi)	35	61	86	112	162	221	290
2002-06 avg CLIPER5 error (n mi)	48	100	160	216	318	419	510
2002-06 avg error relative to CLIPER5 (%)	-26	-39	-46	-48	-49	-47	-43
2002-06 average official bias vector ($^{\circ}$ /n mi $^{-1}$)	309/6	316/14	322/21	324/27	321/24	354/19	035/39
2002-06 No. of cases	1852	1686	1519	1362	1100	885	723
2007 official error relative to 2002-06 mean (%)	-7	-16	-18	-17	-9	-24	-10
2007 CLIPER5 error relative to 2002-06 mean (%)	-6	-15	-24	-26	-25	-23	1

the forecast's nominal initial time (0000, 0600, 1200, or 1800 UTC). At the conclusion of the season, forecasts are evaluated by comparing the projected positions and intensities to the corresponding post-storm-derived "best track" positions and intensities for each cyclone. A forecast is included in the verification only if the system is classified in the final best track as a tropical or subtropical cyclone at both the forecast's initial time and at the projection's valid time. All other stages of development [e.g., tropical wave, (remnant) low, extratropical] are excluded. For verification purposes, forecasts from special advisories² do not supersede the original forecast issued for that synoptic time.

It is important to distinguish between forecast error and forecast skill. Track forecast error is defined as the great-circle distance between a cyclone's forecast position and the best-track position at the forecast verification time. Skill, on the other hand, represents a normalization of forecast error against some standard or baseline, and is positive when the forecast error is smaller than the error from the baseline. To assess the degree of skill in a set of track forecasts, the track forecast error can be compared with the error from CLIPER5, a climatology and persistence model that contains no information about the current state of the atmosphere (Neumann 1972; Aberson 1998). Errors from the CLIPER5 model are taken to represent a "no skill" level of accuracy that can be used as a baseline for evaluating other forecasts. If CLIPER5 errors are unusually low during a given season, for example, it indicates that the year's storms were inherently "easier" to forecast than normal or

otherwise unusually well behaved. The current version of CLIPER5 is based on developmental data from 1931 to 2004 for the Atlantic.

Particularly useful skill standards are those that do not require operational products or inputs and can therefore be easily applied retrospectively to historical data. CLIPER5 satisfies this condition, since it can be run using persistence predictors (e.g., the storm's current motion) that are based on either operational or best-track inputs. The best-track version of CLIPER5, which yields substantially lower errors than its operational counterpart, is generally used to analyze lengthy historical records for which operational inputs are unavailable. Forecasters, of course, see only the operational models.

Table 11 presents the results of the NHC official track forecast verification for the 2007 season, along with results averaged for the previous 5-yr period (2002-06). In 2007, the NHC issued 208 tropical cyclone forecasts, a number well below the 5-yr mean from the very active 2002-06 period (about 50% of the 5-yr mean at 12 h and about 15% of the 5-yr mean at 120 h). Two storms (Dean and Noel) accounted for all of the 120-h forecasts. Mean track errors ranged from 33 n mi at 12 h to 258 n mi at 120 h. Mean official track forecast errors were smaller in 2007 than during the previous 5-yr period (by 7%-24%), and in fact, the 36-96-h forecast projections established new all-time lows. Since 1990, 24-72-h track forecast errors have been reduced by a little more than 50% (Franklin 2009).

Substantial vector biases at the longer ranges were noted in 2007; at 120 h, the official forecast bias was 162 n mi to the east-northeast of the verifying position. These vector biases largely were caused by forecasts for Hurricane Dean that had a persistent slow (and slightly northward) bias. Track forecast skill in 2007 was comparable to skill levels over the previous 5-yr period (Table 11).

² Special advisories are issued whenever an unexpected significant change has occurred or when U.S. watches or warnings are issued between regularly scheduled advisories. The current practice of retaining and verifying the original advisory forecast began in 2005.

TABLE 12. Homogenous comparison of official and DSHIFOR5 intensity forecast errors in the Atlantic basin for the 2007 season for all tropical and subtropical cyclones. Long-term averages are shown for comparison.

	Forecast period (h)						
	12	24	36	48	72	96	120
2007 avg official error (kt)	8.1	11.0	14.0	17.9	23.5	28.6	30.0
2007 avg DSHIFOR5 error (kt)	9.8	12.6	17.4	23.5	29.8	39.0	42.7
2007 avg error relative to DSHIFOR5 (%)	-17	-13	-20	-24	-21	-27	-30
2007 official bias (kt)	-0.5	-1.1	-1.3	-0.4	-1.4	-4.5	-12.6
2007 No. of cases	177	145	116	93	62	39	23
2002-06 avg official error (kt)	6.4	9.8	12.0	14.1	18.3	19.8	21.8
2002-06 avg DSHIFOR5 error (kt)	7.6	11.5	14.8	17.6	21.3	23.7	24.3
2002-06 avg error relative to DSHIFOR5 (%)	-16	-15	-19	-20	-14	-17	-10
2002-06 official bias (kt)	0.3	0.7	0.5	0.0	-0.2	-1.0	-0.8
2002-06 No. of cases	1852	1686	1519	1362	1100	885	723
2007 official error relative to 2002-06 mean (%)	26	12	17	27	28	44	38
2007 DSHIFOR5 error relative to 2002-06 mean (%)	29	10	18	34	40	65	76

Forecast intensity error is defined as the absolute value of the difference between the forecast and best-track intensity at the forecast verifying time. Skill in a set of intensity forecasts is assessed using version 5 of the Decay-Statistical Hurricane Intensity Forecast model (Decay-SHIFOR5, or DSHIFOR5 hereinafter). The DSHIFOR5 forecast is obtained by initially running SHIFOR5, the climatology and persistence model for intensity that is analogous to the CLIPER5 model for track (Jarvinen and Neumann 1979; Knaff et al. 2003). The output from SHIFOR5 is then adjusted for land interaction by applying the decay rate of DeMaria et al. (2006). The application of the decay component requires a forecast track, which here is given by CLIPER5. The use of DSHIFOR5 as the intensity skill benchmark was introduced in 2006. On average, DSHIFOR5 errors are about 5%–15% lower than SHIFOR5 in the Atlantic basin from 12 to 72 h, and about the same as SHIFOR5 at 96 and 120 h.

Table 12 present the results of the NHC official intensity forecast verification for the 2007 season, along with results averaged for the preceding 5-yr period. Mean forecast errors in 2007 ranged from about 8 kt at 12 h to nearly 30 kt at 96 and 120 h. These errors were considerably above the 5-year means—by 25% or more at all time periods except 24 and 36 h. Large negative forecast biases (i.e., underforecasts of intensity) occurred at 96 and 120 h, and the biases were negative at all time periods. In contrast, long-term intensity forecast biases are near zero. These large errors and negative biases are likely due in part to the fact that the season had many instances of rapid strengthening³ (11.9% of all

24-h intensity changes qualified, which is more than twice the climatological rate, and nearly 4 times the rate observed in 2006). This led to DSHIFOR errors that were well above normal; in short, this year's storms posed unusual forecast challenges.

Additional information on verification of NHC official forecasts, as well as for forecast guidance, is provided by Franklin (2009).

A hurricane (tropical storm) warning is defined by NHC as notice that 1-min sustained winds of hurricane (tropical storm) force are expected in the warning area within the next 24 h. A watch means the conditions are possible within 36 h. Table 13 shows the watch and warning lead times for cyclones that affected the United States in 2007. The lead time is defined as the time between the issuance of the watch or warning and the time of landfall or the closest point of approach of the cyclone center to the coastline. However, this definition will usually result in an overestimation of lead times for preparedness actions, particularly for hurricanes, as tropical storm conditions can arrive several hours prior to the onset of hurricane conditions. Table 13 includes only the most significant landfall for each cyclone and verifies only the strongest conditions that occurred. The issuance of watches and/or warnings for territories outside of the United States is the responsibility of their respective governments, and those statistics are not presented here. While watch and warning lead time goals were generally met for Erin and Gabrielle, the lead time for the warning associated with Barry was less than 24 h, and no watch was issued prior to the issuance of the warning, since the cyclone developed within 24 h of landfall. The warning lead times were poorest for Humberto, with only 16 h of lead time for the tropical storm warning, and only 2 h for the hurricane warning. Watches were not issued prior to the warnings due to the unexpectedly rapid development of that cyclone off the Texas coast.

³ Rapid intensification is defined here as a 30-kt-or-greater increase in maximum winds in a 24-h period, following Kaplan and DeMaria (2003). This threshold corresponds to the fifth percentile of all intensity changes in the Atlantic basin.

TABLE 13. Watch and warning lead times (see text) for tropical cyclones affecting the United States in 2007. For cyclones with multiple landfalls, the most significant is given. If multiple watch–warning types were issued, the type corresponding to the most severe conditions experienced over land is given.

Storm	Landfall or point of closest approach	Watch–warning type (H–TS)	Watch lead time (h)	Warning lead time (h)
Barry	Tampa Bay, FL	TS		17
Erin	Lamar, TX	TS	57	21
Gabrielle	Cape Lookout National Seashore, NC	TS	36	24
Humberto	High Island, TX	TS H		16 2

Acknowledgments. The cyclone summaries are based on reports prepared by the second and third authors and the following other hurricane specialists at the National Hurricane Center: Lixion Avila, Jack Beven, Eric Blake, Daniel Brown, James Franklin, Richard Pasch, and Jamie Rhome. These reports are also available online (<http://www.nhc.noaa.gov/2007atlan.shtml>). Ethan Gibney of I. M. Systems Group at the NOAA/National Climatic Data Center in Asheville, NC, prepared the track map. Much of the U.S. impact information presented in the storm summaries was compiled by local NWS Weather Forecast Offices. Information on impacts and observations for areas outside the United States were provided by meteorological agencies of the respective countries. Thanks are given to an anonymous reviewer who provided comments that helped improve this manuscript.

REFERENCES

- Aberson, S. D., 1998: Five-day tropical cyclone track forecasts in the North Atlantic basin. *Wea. Forecasting*, **13**, 1005–1015.
- , and J. L. Franklin, 1999: Impact on hurricane track and intensity forecasts of GPS dropwindsonde observations from the first season flights of the NOAA Gulfstream-IV jet aircraft. *Bull. Amer. Meteor. Soc.*, **80**, 421–427.
- Bell, G. D., and Coauthors, 2000: Climate assessment for 1999. *Bull. Amer. Meteor. Soc.*, **81**, S1–S50.
- , E. Blake, C. W. Landsea, S. B. Goldenberg, R. Pasch, and T. Kimberlain, 2008: Tropical cyclones—Atlantic basin. *Bull. Amer. Meteor. Soc.*, **89**, S68–S71.
- Brennan, M. J., C. C. Hennon, and R. D. Knabb, 2009: The operational use of QuikSCAT ocean surface vector winds at the National Hurricane Center. *Wea. Forecasting*, **24**, 621–645.
- Brueske, K. F., and C. S. Velden, 2003: Satellite-based tropical cyclone intensity estimation using the NOAA-KLM series Advanced Microwave Sounding Unit (AMSU). *Mon. Wea. Rev.*, **131**, 687–697.
- DeMaria, M., and J. Kaplan, 1994: A Statistical Hurricane Intensity Prediction Scheme (SHIPS) for the Atlantic basin. *Wea. Forecasting*, **9**, 209–220.
- , J. A. Knaff, and J. Kaplan, 2006: On the decay of tropical cyclone winds crossing narrow landmasses. *J. Appl. Meteor.*, **45**, 491–499.
- Demuth, J. L., M. DeMaria, and J. A. Knaff, 2006: Improvement of Advanced Microwave Sounding Unit tropical cyclone intensity and size estimation algorithms. *J. Appl. Meteor. Climatol.*, **45**, 1573–1581.
- Dvorak, V. E., 1984: Tropical cyclone intensity analysis using satellite data. NOAA Tech. Rep. NESDIS 11, 47 pp.
- Franklin, J. L., cited 2009: 2007 National Hurricane Center Forecast Verification Report. [Available online at http://www.nhc.noaa.gov/verification/pdfs/Verification_2007.pdf.]
- , and D. P. Brown, 2008: Atlantic hurricane season of 2006. *Mon. Wea. Rev.*, **136**, 1174–1200.
- Hawkins, J. D., T. F. Lee, J. Turk, C. Sampson, J. Kent, and K. Richardson, 2001: Real-time Internet distribution of satellite products for tropical cyclone reconnaissance. *Bull. Amer. Meteor. Soc.*, **82**, 567–578.
- Hebert, P. J., and K. O. Poteat, 1975: A satellite classification technique for subtropical cyclones. NOAA Tech. Memo. NWS SR-83, 25 pp. [Available from National Weather Service, Fort Worth, TX 76102.]
- Jarvinen, B. R., and C. J. Neumann, 1979: Statistical forecasts of tropical cyclone intensity for the North Atlantic basin. NOAA Tech. Memo. NWS NHC-10, 22 pp.
- Kalnay, E., and Coauthors, 1996: The NCEP/NCAR 40-Year Reanalysis Project. *Bull. Amer. Meteor. Soc.*, **77**, 437–471.
- Kaplan, J., and M. DeMaria, 2003: Large-scale characteristics of rapidly intensifying tropical cyclones in the North Atlantic basin. *Wea. Forecasting*, **18**, 1093–1108.
- Knaff, J. A., M. DeMaria, B. Sampson, and J. M. Gross, 2003: Statistical, 5-day tropical cyclone intensity forecasts derived from climatology and persistence. *Wea. Forecasting*, **18**, 80–92.
- Neumann, C. B., 1972: An alternate to the HURRAN (hurricane analog) tropical cyclone forecast system. NOAA Tech. Memo. NWS SR-62, 24 pp.
- NWS, cited 2009: National Weather Service glossary. [Available online at <http://www.weather.gov/glossary/>.]
- Saffir, H. S., 1973: Hurricane wind and storm surge. *Military Eng.*, **423**, 4–5.
- Simpson, R. H., 1974: The hurricane disaster potential scale. *Weatherwise*, **27**, 169–186.
- Uhlhorn, E. W., P. G. Black, J. L. Franklin, M. Goodberlet, J. Carswell, and A. S. Goldstein, 2007: Hurricane surface wind measurements from an operational stepped frequency microwave radiometer. *Mon. Wea. Rev.*, **135**, 3070–3085.